

8-2021

Vascular Disease Pathogenesis in Smooth Muscle Dysfunction Syndrome and Majewski Osteodysplastic Primordial Dwarfism Type II

Jamie Wright

Follow this and additional works at: https://digitalcommons.library.tmc.edu/utgsbs_dissertations

 Part of the [Medical Cell Biology Commons](#), [Medical Genetics Commons](#), and the [Medical Molecular Biology Commons](#)

Recommended Citation

Wright, Jamie, "Vascular Disease Pathogenesis in Smooth Muscle Dysfunction Syndrome and Majewski Osteodysplastic Primordial Dwarfism Type II" (2021). *The University of Texas MD Anderson Cancer Center UTHealth Graduate School of Biomedical Sciences Dissertations and Theses (Open Access)*. 1116.

https://digitalcommons.library.tmc.edu/utgsbs_dissertations/1116

This Dissertation (PhD) is brought to you for free and open access by the The University of Texas MD Anderson Cancer Center UTHealth Graduate School of Biomedical Sciences at DigitalCommons@TMC. It has been accepted for inclusion in The University of Texas MD Anderson Cancer Center UTHealth Graduate School of Biomedical Sciences Dissertations and Theses (Open Access) by an authorized administrator of DigitalCommons@TMC. For more information, please contact digitalcommons@library.tmc.edu.

Vascular Disease Pathogenesis in Smooth Muscle Dysfunction Syndrome and
Majewski Osteodysplastic Primordial Dwarfism Type II

by

Jamie Mae Wright, B.S.

APPROVED:

Dianna M. Milewicz, M.D., Ph.D.
Advisory Professor

Jaroslav Aronowski, M.D., Ph.D.

Ruth Heidelberger, M.D., Ph.D.

Louise McCullough, MD, PhD

Guang Peng, M.D., Ph.D.

APPROVED:

Dean, The University of Texas
MD Anderson Cancer Center UTHHealth Graduate School of Biomedical Sciences

Vascular Disease Pathogenesis in Smooth Muscle Dysfunction Syndrome and
Majewski Osteodysplastic Primordial Dwarfism Type II

A

Dissertation

Presented to the Faculty of

The University of Texas

MD Anderson Cancer Center UTHealth

Graduate School of Biomedical Sciences

in Partial Fulfillment

of the Requirements

for the Degree of

Doctor of Philosophy

by

Jamie Mae Wright, B.S.

Houston, Texas

August 2021

Acknowledgements

I would like to thank my advisor, Dianna Milewicz, for your support and faith over the years. The past six years have been some of the most challenging of my life, but you never gave up on me and were a constant source of support. Thank you for pushing me and helping me to grow as a scientist and a person.

I would like to thank all my committee members over the years for your support, encouragement, ideas, insights, and mentorship. I would especially like to thank my Supervisory Committee Members: Ruth Heidelberger, Louise McCullough, Jaroslaw Aronowski, Guang Peng, and Robert Bryan. Thank you for helping to further my science while also providing much-needed advice and mentorship over the years.

Thank you to all those who have helped me over the years in the lab, your assistance and guidance has been invaluable to these projects and to my growth as a scientist. Thank you Shao-Qing Kuang for helping me to get started on the MOPDII project and for your patient guidance as I started in the lab. Special thanks to Airu Niu for your technical assistance with experiments. Thank you Jiyuan Chen for answering my endless questions and always being willing to show me new techniques. Thank you to Alexa Janda, Ping Zhou, Amelie Pinard, and Anita Kaw for your friendship, support, and always being willing to proofread and talk through concerns. Special thanks to Abhi Chattopadhyay and Kaveeta Kaw for helping with experiments and helping take my project in this new and exciting direction. Special thanks also to Callie Kwartler your support, guidance, and pep talks have been invaluable over these past six years.

Also a special thanks to all the doctors who have helped me get through the past six years with care and compassion. Thanks especially to Dr. Holly Varner for not only caring for me for a patient, but as a person. You are the type of doctor I aspire to be for my patients. And thank you to Dr. David Sandberg, you quite literally saved my brain. Thank you David for being a friend and mentor, and for providing me with amazing, invaluable, and memorable experiences in Haiti.

Last but certainly not least, thank you to my family. Thank you mom for driving across Texas countless times to be with me during surgeries and hospitalizations. Thank you for always being a listening ear and for guiding me to the person I am today. Thank you dad for your being a listening ear and always being there with support, encouragement, and praise. Thank you Maggie for being a steady voice of reason when I am stressed and for the endless prayers and encouragement. Thank you Carrie for always building me up and continually encouraging me along the way. Thank you Amber for being like a sister to me here in Houston, always including me as part of your family and being there with a silly joke when I need a laugh. And thank you Chris and Elizabeth Janda, you have treated me like one of your own, always there to help and support me. I am beyond blessed to have the love and support of so many people on this journey. Thank you.

Vascular Disease Pathogenesis in Smooth Muscle Dysfunction Syndrome and Majewski Osteodysplastic Primordial Dwarfism Type II

Jamie Mae Wright, B.S.

Advisory Professor: Dianna M. Milewicz, M.D., Ph.D.

Vascular diseases are a leading cause of morbidity and mortality world-wide. Understanding their pathogenesis is crucial to better diagnosis and management of these life-threatening conditions. Through the study of rare mutations that lead to early onset and severe vascular diseases, we can elucidate underlying mechanisms for vascular disease pathogenesis and develop better treatments to prevent and manage more common causes of vascular diseases. In this study we look at two rare diseases that lead to severe vascular phenotypes, Smooth Muscle Dysfunction Syndrome (SMDS) and Majewski Osteodysplastic Primordial Dwarfism Type II (MOPDII). SMDS is a rare condition due to pathogenic variants in *ACTA2* p.Arg179, which lead to dysfunction of smooth muscle cells (SMCs) throughout the body. Complications of SMDS include early-onset thoracic aortic aneurysms and dissections, moyamoya-like cerebrovascular disease, patent ductus arteriosus, pulmonary hypertension and poorly characterized pulmonary disease, hypoperistalsis of the gut, hypotonic bladder, and congenital mydriasis. Here lung and liver pathology findings from two infants and one adult with SMDS are described, including thickening of the terminal branches of the hepatic artery and

emphysematous pulmonary changes, along with previously described changes consistent with pulmonary arterial hypertension. These data provide further insight into the pathophysiology of complications of SMDS. MOPDII is due to homozygous loss-of-function mutations in *PCNT*, which lead to primordial dwarfism and early onset occlusive vascular disease, including moyamoya disease and coronary artery disease. We examine the pathogenic mechanisms of vascular disease in MOPDII using a novel SMC-specific pericentrin knock-out mouse line (*Pcnt^{SMKO}*). Using this mouse model, we identify increased proliferation of SMCs explanted from the aortas of *Pcnt^{SMKO}* mice and activation of the ataxia telangiectasia and rad3 related (ATR) cell cycle regulation pathway. Further, we identify phenotypic modulation of *Pcnt^{SMKO}* SMCs *in vitro* to a phenotype similar to that observed with the progression of atherosclerosis in mice. The modulated cells express markers of both macrophages and fibroblasts, with a reduction in SMC identity markers. This phenotypic modulation in *Pcnt^{SMKO}* SMCs is associated with activation of the unfolded protein response and cytosolic stress pathways. The findings presented here suggest potential mechanisms and future targets for vascular disease intervention.

Table of Contents

Approvals

Title Page

Acknowledgments.....iii

Abstract.....v

Table of Contents.....vii

List of Illustrations.....ix

List of Tables.....xi

CHAPTER ONE: Introduction.....1

 The Artery Wall.....2

 Genetically-Triggered Vascular Disease.....4

 Vascular Smooth Muscle Cells.....14

 Signaling Pathways Regulating SMC Differentiation.....17

 Atherosclerosis.....18

 Phenotypic Modulation in SMCs.....20

CHAPTER TWO: Liver and lung pathology in patients with Multisystemic

 Smooth Muscle Dysfunction Syndrome due to ACTA2 pathogenic
 variants disrupting R179.....23

 Introduction.....24

 Materials and Methods.....25

 Results.....26

 Discussion.....31

CHAPTER THREE: Smooth muscle cell specific knock-out of Pcnt leads to phenotypic modulation <i>in vitro</i> and atherosclerotic disease <i>in vivo</i>	35
Introduction.....	36
Materials and Methods.....	43
Results.....	53
Discussion.....	68
CHAPTER FOUR: Discussion.....	72
References.....	79
Vita.....	97

List of Illustrations

Figure 1.1: Layers of the artery wall.....	2
Figure 1.2: Embryonic origins of SMCs in the aorta.....	16
Figure 1.3: Phenotypic switching of vascular smooth muscle cells.....	17
Figure 1.4: Current knowledge of identity and origins of vascular smooth muscle cells	21
Figure 2.1: Thickening of the terminal branches of the hepatic artery, expansion of the portal tracts, and non-alcoholic hepatic steatosis in 6- and 22-month-old infants and a 32-year-old adult with SMDS.....	29
Figure 2.2: All three SMDS patients exhibit severe lung changes consistent with pulmonary hypertension and emphysematous changes.....	30
Figure 3.1: Role of pericentrin in the ATR-Chk1 pathway.....	38
Figure 3.2: Pcmt-flox mouse construct and resulting cross into SMA-CreER ^{T2} mice.....	45
Figure 3.3: Left anterior descending coronary artery from MOPDII patient 1.....	55
Figure 3.4: Left main coronary artery bifurcation of MOPDII patient 2.....	56
Figure 3.5: Construct of Pcmt-flox mouse and confirmation of reduction in pericentrin expression.....	57
Figure 3.6: Contractile protein expression in Pcmt ^{SMKO} SMCs.....	58
Figure 3.7: Pcmt ^{SMKO} (Pcmt ^{fl/fl} +4OHT) cells display increased proliferation and migration compared to DMSO treated control cells.....	59
Figure 3.8: Activation of the ATR-Chk1 pathway in Pcmt ^{SMKO} SMCs.....	61
Figure 3.9: 4OHT treated Pcmt ^{SMKO} cells display phenotypic switching.....	62

Figure 3.10: Pcnt ^{SMKO} cells undergo phenotypic modulation to a fibroblast- and mesenchymal-like state.....	63
Figure 3.11: Pcnt ^{SMKO} cells show activation of Unfolded Protein Response (UPR) pathways.....	64
Figure 3.12: Cytosolic stress pathways are significantly elevated at baseline in 4OHT-treated Pcnt ^{SMKO} SMCs compared to DMSO-treated control cells.....	65
Figure 3.13: Pcnt ^{SMKO} mice do not have aortic dilatation or cardiac dysfunction on echocardiography.....	66
Figure 3.14: Atherosclerotic disease in Pcnt ^{SMKO} mice following AAV-PCSK9 ^{DY} and high fat diet.....	68

List of Tables

Table 3.1: List of antibodies used for Western blot.....47

Table 3.2: List of SYBR primers used for quantitative real-time PCR (qPCR).....48

Chapter 1: Vascular Smooth Muscle Cells and Genetically-Trigged Vascular Disease

The Artery Wall

Artery walls are composed of three main layers, from outside to in: the *tunica adventitia*, *tunica media*, and *tunica intima* (figure 1.1) (Milewicz et al., 2008; El-Hamamsy and Yacoub, 2009). The tunica adventitia lies outside the external elastic lamina and is comprised primarily of fibroblasts in a collagen-rich extracellular matrix, which functions to help prevent vessel rupture (Milewicz et al., 2008; El-Hamamsy and Yacoub, 2009). In larger arteries such as the aorta, the adventitial layer also contains vaso vasorum, small arteries which provide oxygen and nutrients to the outer layers of the vessel wall (El-Hamamsy and Yacoub, 2009). The tunica media is a thick layer comprised primarily of vascular smooth muscle cells (Milewicz et al., 2008; El-Hamamsy and Yacoub, 2009). Finally, the tunica intima is comprised of a single layer of endothelial cells on a basement membrane of collagen (Milewicz et al., 2008; El-Hamamsy and Yacoub, 2009; Wagenseil and Mecham, 2009).

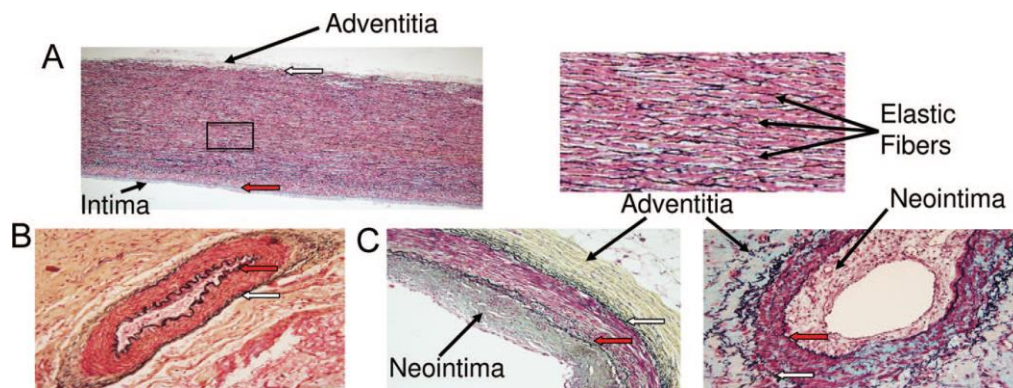


Figure 1.1. Layers of the artery wall. The artery wall consists of three layers, the inner most layer, the intima, lies closest to the artery lumen (A). Going outward, this is followed by the internal elastic lamina (C, red arrow) and then the medial layer made up of SMCs. In elastic arteries, such as the aorta, the SMCs are interposed with multiple layers of elastic fibers (A, inset). This is followed by the external elastic lamina (C, white arrow), and finally the outermost layer, the adventitia (A). In different disease states a neointima can form, extending into the vessel lumen (C). [Used with permission from Milewicz et al, Genetics in Medicine, 2010.]

Vascular smooth muscle cells (SMCs) normally reside primarily in the medial layer where they function to control peripheral blood pressure through their ability to contract and relax (Milewicz et al., 2017). In addition, SMCs produce extracellular matrix components, including collagen, elastin, fibrillin and fibulin, which provide resistance to the high pressures of circulating blood (El-Hamamsy and Yacoub, 2009; Frismantiene et al., 2018). Collagen provides tensile strength to the media and adventitia to resist vessel rupture, while elastin allows the artery wall to stretch, distributing pressure and retaining the overall vessel shape (El-Hamamsy and Yacoub, 2009). In turn, elastin interacts with SMCs to regulate cytoskeletal structure by inhibiting the SMC proliferative, synthetic phenotype, keeping them in a differentiated, contractile state (El-Hamamsy and Yacoub, 2009; Milewicz et al., 2010a). Elastin content differentiates two main artery types, elastic arteries and muscular arteries. Large elastic arteries, such as the aorta, have a medial layer made up of alternating layers of elastin and SMCs lined up end-to-end. Muscular arteries, such as those in the brain, contain only two elastin layers separating the adventitia from the media, the external elastic lamina, and the media from the intima, the internal elastic lamina. Those arteries most proximal to the heart tend to be elastic with a medial layer comprised of vascular smooth muscle cells sandwiched between layers of elastin fibers and surrounded by extracellular matrix proteins (Milewicz et al., 2008; El-Hamamsy and Yacoub, 2009). Through these lamellar units, the medial layer provides tensile strength and elastic recoil to the vessel wall allowing it to distribute the force of blood flow and retain its shape (Milewicz et al.,

2008; El-Hamamsy and Yacoub, 2009). Moving distally from the heart, arteries transition from elastic to muscular (Yu and Mceniery, 2020).

Within the medial layer, SMCs form an elastin-contractile unit through connection with elastin fibers surrounded by microfibrils (Karimi and Milewicz, 2016). On the surface of SMCs are focal adhesion complexes through which microfibrils bind to integrin receptors on the cell surface (Karimi and Milewicz, 2016). These focal adhesion complexes in turn link to the SMC contractile filaments inside the cell (Karimi and Milewicz, 2016). These SMC elastin-contractile serve to transmit forces from the elastin fibers to the SMC (Karimi and Milewicz, 2016).

Genetically-Triggered Vascular Disease

Cardiovascular disease is currently the most common cause of death worldwide (Francula-Zaninovic and Nola, 2018; Frismantiene et al., 2018; Arnett et al., 2019). Coronary artery disease and stroke, both a result of pathologic narrowing of the vessel lumen, account for most of these deaths (Frismantiene et al., 2018). Common risk factors for cardiovascular disease include some invariable factors such as age and family history, and variable risk factors, including smoking, level of physical activity, hypertension, obesity, hyperlipidemia, and diabetes mellitus (Francula-Zaninovic and Nola, 2018).

Vascular disease that is early-onset and arises independently of risk factors known to lead to cardiovascular disease may be genetically-triggered. Single gene mutations have been identified that predispose to vascular pathology, including coronary artery disease, stroke, aortic aneurysms and dissections, cerebral aneurysms, and Moyamoya disease. Some of these mutations will be discussed in

the sections below. By studying these rare genetic variants, we are not only able to identify pathways important to these rare diseases, but also to delineate the cellular pathways underlying more common causes of vascular pathology. Genes affecting each layer and cell type of the artery wall have been identified (Munot et al., 2011). For the purpose of these studies, we focused on mutations in two genes that cause diffuse and diverse vascular pathology, *ACTA2* and *PCNT*.

I. Thoracic Aortic Aneurysms and Dissections

Thoracic aortic aneurysms and dissections (TAAD) describe a group of conditions affecting the large, main artery emanating from the heart, the aorta. TAAD accounts for 43,000 to 47,000 deaths worldwide each year (Pinard et al., 2019). The pathologic hallmark of this set of conditions is termed “medial degeneration”, characterized by the loss or fragmentation of elastic fibers and accumulation of proteoglycan in the medial layer of the aortic wall (Milewicz et al., 2008). As depicted in figure 1.2, TAAD can affect either the ascending aorta, descending aorta, or both (Milewicz et al., 2008). Dissection is often, but not always, preceded by aneurysmal expansion of the artery wall. Dissection occurs when a break or opening develops in the vessel wall allowing blood into a false lumen which can obstruct flow through the vessel or rupture leading to hemorrhage.

Multiple genetic syndromes can predispose individuals to TAAD, including Marfan syndrome caused by mutations in *FBN1*, Loeys-Dietz syndromes caused by mutations in TGF- β 2 (*TGFB2*) and its receptors (*TGFBR1* and *TGFBR2*), and the vascular form of Ehlers-Danlos syndrome caused by mutations in *COL3A1*, but they account for only 5% of cases (Byers et al., 1981; Mizuguchi et al., 2004; Loeys et al.,

2006; Boileau et al., 2012; Faggion Vinholo et al., 2019; Pinard et al., 2019). At least 20% of non-syndromic TAAD is due to an autosomal dominantly inherited genetic predisposition with decreased penetrance and a variable degree of expression (Albornoz et al., 2006; Guo et al., 2007). Some of the genes involved in non-syndromic TAAD include genes related to the extracellular matrix, such as LOX (Guo et al., 2016; Faggion Vinholo et al., 2019). Genes encoding structural proteins in the SMC contractile unit are also associated with TAAD, including *ACTA2*, *MYH11*, *MYLK*, and *PRKG1* (Zhu et al., 2006; Seol et al., 2010; Guo et al., 2013; Karimi and Milewicz, 2016; Pinard et al., 2019).

II. Moyamoya Disease

Moyamoya refers to a rare cerebrovascular condition in which there is progressive stenosis or narrowing of the intracerebral internal carotid arteries and their proximal branches predisposing to ischemic stroke [Scott and Smith, 2009]. Under normal conditions, these arterial changes in turn lead to the formation of compensatory collateral vessels which look like a “puff of smoke” on cerebral angiogram, from which the name “moyamoya” is derived (Scott and Smith, 2009). Those individuals who have a characteristic vasculopathy in the setting of a condition known to be associated with moyamoya are said to have moyamoya syndrome (Scott and Smith, 2009; Guey et al., 2015). While those individuals with no known risk factors are characterized as having moyamoya disease, which is thought to be multifactorial and polygenic (Scott and Smith, 2009; Guey et al., 2015).

Genetic factors are strongly suspected in Moyamoya Disease based on 10% of cases being familial, a high rate of disease concordance in monozygotic twins and

a strong ethnicity-related effect (Guey et al., 2015). *RNF213* was the first Moyamoya Disease susceptibility gene identified in patients of Japanese descent (Kamada et al., 2011; Liu et al., 2011). Alternatively, genes have been associated with Moyamoya Syndrome leading to moyamoya angiopathy with other neurological and/or non-neurological findings (Guey et al., 2015). These include recessive X-linked loss of expression of *BRCC3/MTCP1* leading to a syndrome of bilateral moyamoya angiopathy, short stature, facial dysmorphism, cardiomyopathy, and hypergonadotropic hypogonadism (Hervé et al., 2010; Miskinyte et al., 2011; Guey et al., 2015). Another identified syndrome due to mutations in *GUCY1A3* associated with unilateral or bilateral moyamoya angiopathy in addition to achalasia leading to regurgitation, arterial hypertension, vasomotor dysfunction, erectile dysfunction, and low platelet count (Hervé et al., 2014; Guey et al., 2015). Finally, some mutations in *ACTA2*, including those leading to Smooth Muscle Dysfunction Syndrome are associated with a moyamoya-like angiopathy associated with diffuse smooth muscle cell abnormalities, including hypotonic bladder, aortic aneurysm and dissection, and pulmonary abnormalities (Guo et al., 2009; Milewicz et al., 2010b; Munot et al., 2012).

III. Coronary Artery Disease

Coronary artery disease (CAD) is characterized by the build-up of atherosclerotic plaque within the coronary arteries, the vessels supplying blood flow to the heart (Khera and Kathiresan, 2017). Despite significant improvements in prevention and treatment in CAD it remains the leading cause of death worldwide (Khera and Kathiresan, 2017). Several environmental factors contribute to the

development of coronary artery disease, including hyperlipidemia, hypertension, diabetes, and smoking (Malakar et al., 2019). Some Mendelian disorders have been associated with CAD, including familial hypercholesterolemia, which led to the development of novel therapies from the prevention of CAD (Malakar et al., 2019). The most notable of these are hydroxymethylglutaryl-coenzyme A (HMG-CoA) inhibitors, or statins, which inhibit the rate-limiting step in cholesterol biosynthesis (Ward et al., 2019). Other single gene disorders associated with hypercholesterolemia and CAD include mutations in the LDL receptor genes and in proprotein convertase subtilisin/kexin type 9 (PCSK9), which sequester LDL receptors for degradation thus reducing LDL cholesterol levels within the cell (Ogura, 2018; Malakar et al., 2019). These include mutations in low density lipoprotein receptor, LDLR, apolipoprotein A-V, APOA5, and proprotein convertase subtilisin/kexin type 9, PCSK9, which predispose to coronary artery disease (Lehrman et al., 1985; Soria et al., 1989; Abifadel et al., 2003; Musunuru and Kathiresan, 2019).

In response to statins, cells increase the number of low-density lipoprotein receptors. One way the cell counteracts this increase in LDL receptors is through overexpression of PCSK9 (Ogura, 2018). To combat this effect, PCSK9 inhibitors have been developed to prevent the degradation of LDL receptors. In combination with statins, PCSK9 inhibitors have been shown to lower LDL cholesterol and reduce plaque burden (Ogura, 2018).

IV. *ACTA2* and Multisystemic Smooth Muscle Dysfunction Syndrome

Smooth muscle alpha actin (SMA), encoded by *ACTA2*, makes up 40% of the total protein within SMCs and 70% of the total actin making it the most abundant protein in SMCs (Guo et al., 2007). Mutations in *ACTA2* are responsible for as much as 21% of inherited thoracic aortic aneurysms and dissections and that some *ACTA2* mutations lead to a widespread vascular phenotype (Guo et al., 2009). Our laboratory originally identified mutations in *ACTA2* as pathogenic for TAAD.

Smooth muscle cells from patients with mutations in *ACTA2* show multiple abnormalities, including an absence of SMA filaments and large amounts of unpolymerized SMA (Guo et al., 2007). In addition, aortic tissue from these patients had increased proteoglycan content and fragmentation and loss of elastin fibers (Guo et al., 2007). They also displayed an overall reduction in SMC content with occasional areas of increased numbers of disorganized smooth muscle cells. Interestingly, tissue from these patients had abnormal vasa vasorum with thickened medial layers and partial or total occlusion of the vessel lumen by cells staining positive for SMC (Guo et al., 2007).

Mutations in *ACTA2* were originally thought to lead to aneurysmal disease exclusively. The finding of medial thickening in the vasa vasorum along with the observation that patients with mutations in *ACTA2* all had livedo reticularis, a purplish, network-pattern skin discoloration due to constriction or occlusion of deep capillaries in the skin, suggested an occlusive component to the *ACTA2* phenotype (Guo et al., 2007). A study of twenty families, including a total of 127 family members with known heterozygous *ACTA2* mutations revealed striking evidence that mutations in *ACTA2* also lead to early onset vascular occlusive disease (Guo et

al., 2009). For the purpose of these studies, early-onset vascular occlusive disease is defined as disease onset before the age of 55 years in men and before the age of 60 years in women (Guo et al., 2009). As might be expected, TAAD was the primary vascular pathology identified in this cohort (76 of the 127 mutation carriers), but early-onset coronary artery disease (CAD; 26 carriers) and ischemic strokes (15 carriers) were also common findings (Guo et al., 2009). What makes these findings more striking is that none of the family members without a mutation in ACTA2 were affected by TAAD, early-onset CAD or stroke (Guo et al., 2009). Overall, these data found that patients carrying a mutation in ACTA2 were significantly more likely to have premature CAD or stroke than those who did not, drawing a clear link between mutations in ACTA2 and vascular occlusive disease (Guo et al., 2009). Five mutation carriers from families noted to have very early onset strokes (age less than 20 years) had been diagnosed with Moyamoya Disease (Guo et al., 2009).

IV. Majewsky Osteodysplastic Primordial Dwarfism Type II

Microcephalic Primordial Dwarfism (MPD) encompasses a group of disorders characterized by severe pre- and post-natal growth restriction with microcephaly (Bober and Jackson, 2017). Multiple forms of MPD have been identified in the literature (Bober and Jackson, 2017). The most common of these is Majewsky Osteodysplastic Primordial Dwarfism Type II (MOPDII) (Bober and Jackson, 2017). Initially thought to overlap with Seckel Syndrome, which is due to mutations in the ataxia-telangiectasia and Rad3-related (*ATR*) gene, a 2008 study of 25 unrelated individuals with a clinical diagnosis of MOPDII identified PCNT as the underlying mutation in these patients (Griffith et al., 2008; Rauch et al., 2008).

Majewski Osteodysplastic Primordial Dwarfism Type II (MOPDII) is a rare autosomal recessive disorder resulting from loss of function mutations in the gene encoding pericentrin, PCNT (Rauch et al., 2008; Willems et al., 2009). Affected individuals have severe growth restriction beginning *in utero* and persisting postnatally with an average adult height of about 100 cm. Individuals with MOPDII also have severe microcephaly that becomes progressively more disproportionate as patients age (Hall et al., 2004; Bober et al., 2010). MOPDII is distinguishable from other, similar forms of primordial dwarfism by the presence of characteristic bony dysplasia and facial features, and by affected patients having normal or near-normal intelligence (Hall et al., 2004; Willems et al., 2009; Bober et al., 2010).

Individuals with MOPDII have significant morbidity and mortality due to diverse, early-onset vascular diseases, including cerebral aneurysms, Moyamoya Disease (MMD) and coronary artery disease (CAD) (Hall et al., 2004; Brancati et al., 2005; Chen et al., 2014a). The incidence of cerebrovascular disease in these patients, including early onset, rapidly progressive MMD, multiple cerebral aneurysms, and increased vessel tortuosity, has been found to be as high as 19-52% in the published literature (Hall et al., 2004; Bober et al., 2010). Severe, early onset multi-vessel coronary artery disease is another common cause of morbidity and mortality in these patients (Bober et al., 2010). Other vascular findings in patients with MOPDII include bicuspid aortic valve, atrial septal defect, patent ductus arteriosus, myocarditis leading to myocardial infarct, renal artery aneurysms, and pulmonary artery stenosis (Bober et al., 2010). The goal of this study is to elucidate the etiology of the vascular pathology in these patients, which is currently unknown.

MOPDII is associated with loss of function mutations in the gene encoding the centrosome scaffold protein pericentrin, PCNT (Rauch et al., 2008). Through its function in the centrosome, pericentrin is involved in a wide range of cellular activities, including microtubule nucleation, mitotic spindle orientation, and cell cycle regulation. Based on these roles, three main models have been proposed to explain the etiology of the clinical manifestations in patients with MOPDII (Delaval and Doxsey, 2010).

A. Mitotic Spindle Misorientation During Asymmetric Cell Division

During cell division, positioning of the mitotic spindle determines whether a cell divides symmetrically, producing two identical daughter cells, or asymmetrically, producing daughter cells destined for two different cell fates (Alberts et al., 2015). During mitosis pericentrin is localized to the centrosome and acts as a molecular scaffold for the recruitment of other proteins involved in centrosome maturation (Chen et al., 2014). Knocking-out Pcnt in mice leads to misorientation of the mitotic spindle, decreased symmetric cell division in neural progenitor cells, and increased misoriented divisions in fibroblasts (Chen et al., 2014). Decreased symmetric cell division in the neural progenitor pool is hypothesized to cause the microcephaly in these patients (Delaval and Doxsey, 2010; Chen et al., 2014). It is unclear what effect, if any, this would have on the smooth muscle cell population. Vascular smooth muscle cells arise from multiple embryonic origins, but both the cerebral vasculature and the ascending aorta arise via migration from neural crest cell progenitors (Majesky, 2007). A role for asymmetric cell division in smooth muscle

cell differentiation has not been defined. Therefore, this hypothesis will not be pursued in my studies.

B. Microtubule Nucleation Defects

Microtubules (MTs) make up the cell cytoskeleton and are involved in cell growth, movement, and adhesion in addition to determining organelle positioning and cell polarity (Alberts et al., 2015). Pericentrin plays a key role in anchoring the γ -Tubulin Ring Complex (γ -TuRC) for centrosome MT nucleation (Takahashi et al., 2002; Zimmerman et al., 2004; Rauch et al., 2008; Alberts et al., 2015). Radial MTs originating from the centrosome maintain cellular circularity, while MTs originating from sites outside the centrosome, such as the Golgi, provide for directional growth (O'Rourke et al., 2014). During interphase, pericentrin and another centrosome scaffold protein, Cep192, interact in an antagonistic manner to regulate centrosome MT nucleation, with depletion of pericentrin leading to increased centrosome MT nucleation. This increase in centrosome MT nucleation may in turn off-set the balance between radial and directional MT nucleation affecting cell migration (O'Rourke et al., 2014). Vascular smooth muscle cells (SMCs) migrate from the medial layer of the vessel wall into the intima in response to injury (Milewicz et al., 2010; Papke et al., 2013). Therefore, it is possible that loss of pericentrin may in turn lead to defects in SMC migration in response to vessel injury. However, this would likely only play an indirect role in development of vascular occlusive disease; therefore, my studies will focus on cell proliferation and loss of ATR-dependent checkpoint regulation described below.

C. Loss of ATR-Dependent Checkpoint Regulation

Pericentrin has also been found to play a direct role in the regulation of the G2/M checkpoint (Griffith et al., 2008; Delaval and Doxsey, 2010). Checkpoint kinase 1 (Chk1), part of the ataxia telangiectasia and rad3 related (ATR)-dependent DNA damage checkpoint signaling pathway (Figure 1), is anchored to the centrosome by pericentrin (Griffith et al., 2008; Tibelius et al., 2009). Once at the centrosome, Chk1 inhibits G2/M cell cycle progression through deactivation of Cdc25B (Schmitt et al., 2007; Tibelius et al., 2009). In turn, siRNA knock-down of pericentrin in U2OS cells was shown to lead to an increase in the number of cells in late G2 or mitosis (Tibelius et al., 2009). Specifically, in smooth muscle cells, work by Ye and colleagues shows that the Polymerase I inhibitor, CX-5461, decreases neointimal formation via activation of the ATR pathway in SMCs. However, when the ATR pathway is simultaneously inhibited using the ATR inhibitor VE-821, the inhibitory effect of CX-5461 on neointimal formation is abolished (Ye et al., 2017). Interestingly, the primary form of Seckel Syndrome (SCKL1, OMIM #210600), a closely related form of primordial dwarfism often confused with MOPDII, is caused by mutations in ATR. SCKL1 is also associated with vascular pathology including intracranial aneurysms, MMD, and malignant hypertension, although at a lower rate than MOPDII (Galasso et al., 2008; Rahme et al., 2010). These findings suggest that the ATR checkpoint is critically important in regulating smooth muscle cell proliferation and disruption of the ATR pathway via loss of pericentrin may result in aberrant cell proliferation.

Vascular Smooth Muscle Cells

Vascular smooth muscle cells (SMCs) are the main mesenchymal cell type making up the artery wall. Located in the medial layer of the artery wall, smooth muscle cells are organized into lamellar units with SMCs oriented longitudinally between layers of elastin, surrounded by ECM, where they function to regulate blood pressure while also producing extracellular matrix (El-Hamamsy and Yacoub, 2009).

SMCs originate from diverse embryonic origins (figure 1.2). So far eight different embryonic origins have been identified, including the neural crest, proepicardium, somites, and splanchnic mesoderm, among others (Majesky, 2007, 2018). The ascending aorta, aortic arch, and bilateral common carotid arteries all arise from progenitor cells of the neural crest lineage (Majesky, 2007). While the coronary arteries, instead of growing out from the aorta, develop separately from proepicardium progenitors (Majesky, 2007). The boundaries between these embryonic origins are sharply demarcated, although, regardless of origin, SMCs all express the same constellation of differentiation markers, including smooth muscle alpha-actin (SMA, encoded by *ACTA2*), smooth muscle myosin heavy chain (SMMHC, encoded by *MYH11*), calponin (encoded by *CNN1*), and Transgelin (SM22 α , encoded by *TAGLN*) (Majesky, 2007).

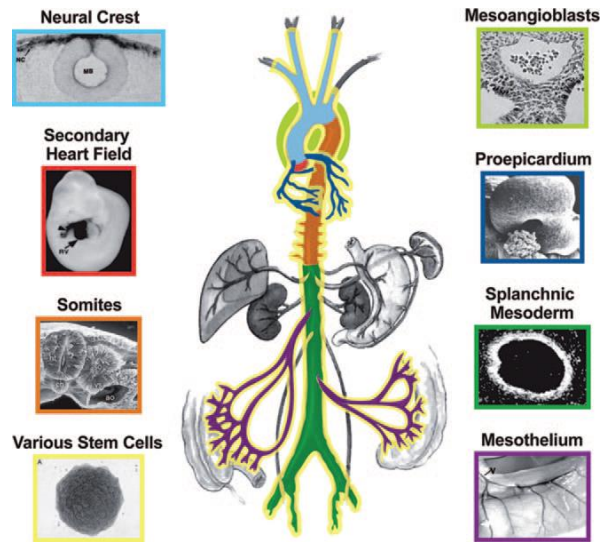


Figure 1.2. Embryonic origins of vascular SMCs in the aorta. From Majesky et al, 2007.

Unlike cardiac myocytes and skeletal muscle, vascular smooth muscle cells are not terminally differentiated and have the unique ability to de-differentiate in response to environmental stimuli (El-Hamamsy and Yacoub, 2009). As mentioned previously, differentiated SMCs express various contractile proteins. In cell culture, SMCs can downregulate these SMC markers and display increased migration, proliferation, and extracellular matrix deposition, so called de-differentiation. SMC differentiation is regulated by the transcription factor serum response factor (SRF) and its cofactor myocardin (Owens et al., 2004; Wang et al., 2018). As the name suggests, myocardin is only expressed in cardiomyocytes and SMCs (Wang et al., 2018). A variety of pathways lead to SRF-myocardin complex formation responding to signals for either proliferation or contractility (Frismantiene et al., 2018; Wang et al., 2018). Once formed, this complex binds to CArG box, which in turn controls expression of SMC-specific genes as well as several immediate-early genes (Wang et al., 2018).

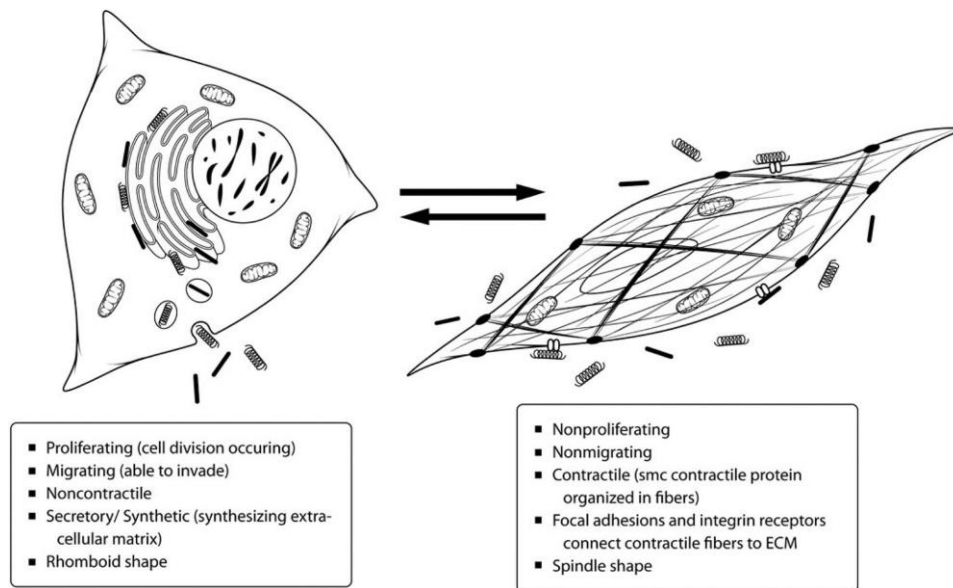


Figure 1.3. Phenotypic switching of vascular smooth muscle cells. SMCs are not terminally differentiated and have the ability to switch between a differentiated, non-proliferative contractile phenotype and a de-differentiated, proliferative synthetic phenotype. [Used with permission from Milewicz et al, Genetics in Medicine, 2010.]

Signaling Pathways Regulating SMC Differentiation

One pathway by which SRF-myocardin may be activated is the TGF- β pathway (Frismantiene et al., 2018). Release of TGF- β is controlled by contraction and relaxation of the ECM (Frismantiene et al., 2018; Michel et al., 2018; Wang et al., 2018). In addition, it is also released during proteolytic activity such as that involving plasmin and matrix metalloproteinases (MMPs). TGF- β induces SMC differentiation through SRF-myocardin. When released, TGF- β acts to regulate SMC interaction with the ECM by increasing the number of focal adhesions on the cell surface through which the cytoskeleton interacts with the ECM (Majesky, 2016; Frismantiene et al., 2018; Wang et al., 2018). Through this feedback interaction on

SMCs, TGF- β serves to regulate the ECM composition (Frismantiene et al., 2018; Michel et al., 2018; Wang et al., 2018).

In addition to myocardin, SRF also interacts with myocardin-related transcription factor (MRTF) (Papke et al., 2013). Unlike myocardin, MRTF shuttles between the cell cytoplasm and the nucleus (Papke et al., 2013). In the cytoplasm, MRTF binds to monomeric actin (Papke et al., 2013). As actin filaments polymerize, MRTF is released revealing a nuclear localization sequence (Papke et al., 2013). In the nucleus, MRTF binds to SRF activating transcription of SMC contractile genes (Papke et al., 2013). When MRTF releases from SRF it is sequestered back to the cytoplasm where it binds to monomeric actin (Papke et al., 2013). Once unbound to MRTF, SRF is free to bind other factors activating SRF-regulated growth responsive genes leading to increased proliferation of SMCs in response to proliferative signals and growth factors (Papke et al., 2013).

The most prominent growth factor influencing SMC proliferation and migration is platelet derived growth factor (PDGF) (Papke et al., 2013). The PDGF family includes four polypeptide chains which combine into five dimeric forms, PDGF-AA, PDGF-AB, PDGF-BB, PDGF-CC, and PDGF-DD (Wang et al., 2018). Of these five, PDGF-BB is the most potent SMC mitogen (Wang et al., 2018). In response to PDGF-BB, SMC migrate to the vessel intima where synthetic SMC may promote pathologic neointimal formation and narrowing of the vessel lumen through excess ECM deposition (Frismantiene et al., 2018).

Atherosclerosis

Atherosclerotic vascular disease is an underlying cause of diverse vascular disease, including heart attack and stroke, making it a contributing factor to the leading cause of death worldwide (Herrington et al., 2016). Atherosclerosis is due to retention of apolipoprotein B-containing lipoproteins in the subendothelial space of the artery wall (Tabas et al., 2015). Lipoproteins are composed of lipid and protein, including low-density lipoproteins (LDL) and high-density lipoproteins (HDL) (Ahotupa, 2017). Lesions develop in specific lesion-prone areas of the artery wall with low or oscillatory endothelial shear stress which contribute to endothelial dysfunction and a susceptibility to lipoprotein retention, this in turn stimulates the entry and differentiation of monocytes into macrophages (Bentzon et al., 2014; Tabas et al., 2015).

In the pre-atherosclerotic stage, termed diffuse intimal thickening, SMCs undergo de-differentiate and migrate from the medial layer to the intimal layer where they produce proteoglycans and elastin, without any lipid deposition (Dubland and Francis, 2016). As the plaque progresses, it accumulates acellular, lipid-rich material with an overlying layer of SMCs and lipid-laden macrophages, termed pathologic intimal thickening (Nakashima et al., 2007; Bentzon et al., 2014). One hypothesis for early atherogenesis is the response-to-retention hypothesis, which posits that “atherogenic lipoproteins are retained in the intima by binding to extracellular proteoglycans” (Williams and Tabas, 1995; Nakashima et al., 2007). These lipoprotein-proteoglycan complexes in turn increase oxidation and lead to uptake by macrophages to form foam cells (Demyanenko and Uzdensky, 2017).

As the plaque progresses macrophages and SMCs invade the lipid-rich core and undergo apoptosis leading to necrotic core development (Bentzon et al., 2014). At this point the lesion is termed a fibroatheroma (Bentzon et al., 2014). New vessels may then grow into the plaque from the vasa vasorum allowing entry of additional monocytes and other immune cells (Bentzon et al., 2014). These new vessels are fragile and leaky, prone to bleeding leading to additional inflammation within the plaque (Bentzon et al., 2014). De-differentiated, synthetic SMCs lay down a matrix of collagen, elastin, and proteoglycan (Bentzon et al., 2014). In addition, calcifications may develop in the plaque forming a fibrocalcific plaque (Bentzon et al., 2014).

The most common cause of thrombosis leading to blockage of a coronary artery and myocardial infarction is plaque rupture (Bentzon et al., 2014). Plaque rupture occurs when there is a defect in a thin fibrous cap allowing the thrombogenic plaque core to come into contact with blood (Bentzon et al., 2014). This thinning is most likely due to loss of synthetic SMCs leading to a reduction in collagen in conjunction with breakdown of the existing collagen matrix by macrophages (Bentzon et al., 2014; Bennett et al., 2016). SMCs from advanced plaques undergo less proliferation with an increased percentage of cells in G1, indicating growth arrest (Bennett et al., 2016). This suggests that SMC proliferation may be protective by reinforcing the fibrous cap (Bennett et al., 2016).

Phenotypic Modulation in SMCs

In addition to SMC's ability to de-differentiate, they also have the ability to undergo a process termed phenotypic modulation in which SMCs take on a macrophage-, fibroblast-, or mesenchymal stem cell (MSC)-like phenotype (Bennett

et al., 2016; Alencar et al., 2020). Complications such as heart attack and stroke arise when an unstable atherosclerotic plaque ruptures (Shankman et al., 2015; Bennett et al., 2016). Plaque stability is at least in part a function of its cellular composition with a thick fibrous cap comprised of SMA-positive SMCs conferring stability (Bennett et al., 2016). Conversely, a thin cap with few SMA-positive cells, large numbers of cells expressing macrophage markers such as *CD68* and *LGALS3*, and a large necrotic core containing lipid-laden foam cells denote plaque instability (Shankman et al., 2015; Bennett et al., 2016).

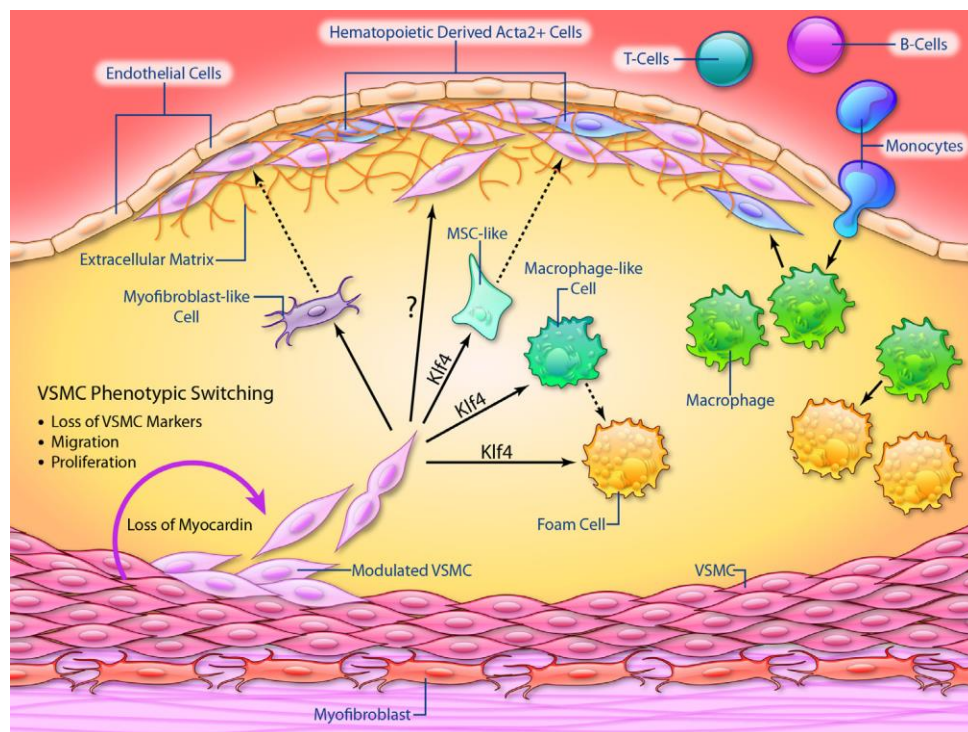


Figure 1.4. Current knowledge of identity and origins of vascular smooth muscle cells. SMCs can also undergo phenotypic modulation to multiple cellular phenotypes, including macrophage-, fibroblast-, and mesenchymal stem cell-like cell populations. This phenotypic modulation is thought to be mediated through the transcription factor Klf4. [From Bennett et al, 2016.]

In the presence of cholesterol, SMCs can undergo a process termed phenotypic modulation, downregulating contractile markers and upregulating markers of macrophages, fibroblasts, and MSCs (Shankman et al., 2015; Wirka et al., 2019; Chattopadhyay et al., 2020). As much as 20-30% of CD68-positive cells within advanced atherosclerotic plaques are of SMCs origin (Shankman et al., 2015; Bennett et al., 2016). These macrophage-like cells differ from traditional macrophages in that they have a reduced phagocytic capacity, which is thought to contribute to a pro-atherosclerotic phenotype by a reduced ability to clear dying cells, lipids, and debris, and by exacerbating inflammation (Bennett et al., 2016).

This downregulation of contractile markers in phenotypically modulated SMCs has been shown to be mediated through the transcription factor KLF4 (Shankman et al., 2015). SMC-specific conditional knockout of *Klf4* resulted in a reduction in lesion size, an increase in lesion stability, and a reduction in SMC-derived MSCs and macrophages (Shankman et al., 2015). These findings suggest that while synthetic SMCs appear to stabilize the fibrous cap, phenotypically modulated SMCs lead to plaque destabilization.

Chapter 2: Liver and lung pathology in patients with Multisystemic Smooth Muscle

Dysfunction Syndrome due to ACTA2 pathogenic variants disrupting R179

Introduction

Heterozygous pathogenic variants in *ACTA2*, encoding smooth muscle α -actin (SMA), *ACTA2*, are responsible for 15% of familial thoracic aortic aneurysms and dissections (Morisaki et al., 2009; Regalado et al., 2015). *De novo*, missense mutations disrupting arginine 179 (*ACTA2* p.Arg179) lead to severe disease termed Smooth Muscle Dysfunction Syndrome (SMDS) that is characterized by patent ductus arteriosus (PDA) or aortopulmonary window (APW), childhood onset of thoracic aortic aneurysms and dissections and moyamoya-like cerebrovascular disease, primary pulmonary arterial hypertension, congenital mydriasis, intestinal hypoperistalsis and malrotation, and hypotonic bladder (SMDS, MIM# 613834) (Milewicz et al., 2010b; Brodsky et al., 2014; Logeswaran et al., 2017; Regalado et al., 2018; Taubenslag et al., 2019).

The clinical complications of SMDS and treatment guidelines have been delineated (PMID: 33199432, Regalado et al., 2018). Early deaths in these patients are due to aortic complications, strokes due to the cerebrovascular disease, and pulmonary complications. Pulmonary disease in patients with SMDS include chronic lung disease and asthma (27%), requirement for respiratory tract agents and/or home oxygen in one-third of patients, and pulmonary arterial hypertension in half of the patients (Regalado et al., 2018). In addition, persistent dilation of the main pulmonary artery and/or its branches, a finding often associated with pulmonary arterial hypertension, is present in half of SMDS patients (Raymond et al., 2014; Regalado et al., 2018). One-third of affected individuals die prematurely of pulmonary complications. Lung histology from one SMDS patient revealed

emphysematous changes in the lung, along with thickening of the arterial walls consistent with pulmonary hypertension (Prabhu et al., 2017). Hepatic complications also occur in SMDS patients, including one infant who died of acute fulminant liver failure, and another who had transiently elevated hepatic transaminases of unknown etiology (Munot et al., 2012).

Aortic and cerebrovascular pathology in patients with mutations in *ACTA2* R179 have been described previously, but limited data are available on the pulmonary and hepatic pathology. Presented here are clinical and histologic findings at autopsy of three unrelated patients with SMDS. The data highlight previously undescribed liver and lung structural abnormalities in these patients.

Materials and Methods

The study protocol was approved by the Institutional Review Board of the University of Texas Health Science Center at Houston and the patient or family members consented to these studies. Pathology slides of the liver and lung were obtained at autopsy from three patients with SMDS. Control tissue was obtained from a 5.5-month-old female who died due to a post-operative sickle cell crisis and a 46-year-old male who died of complications of glioblastoma multiforme. Medical records, including imaging reports, surgical reports, pathology reports, and physicians' notes, were reviewed.

Liver and lung sections from each patient were stained with hematoxylin and eosin (H&E). Wall thickness was calculated using ImageJ software. The outer area, including the media and intima, was measured and the luminal area subtracted.

Percent wall thickness was then calculated by dividing the wall area by the total outer area and calculating the percentage.

Results

Clinical data

Patient 1 is a 6-month-old infant boy with SMDS who inherited the *ACTA2* p.Arg179His mutation from his mother, a 26-year-old with SMDS. The mother had surgical repair of a PDA in infancy and surgical repair of the aortic valve, root, ascending aorta, and an inferior hemiarch for an aortic coarctation at 24 years of age. Fetal echocardiography 5 weeks prior to delivery revealed normal heart size with mild dilation of the main pulmonary artery. The proband was delivered at 37 6/7 weeks via uncomplicated, planned cesarean section. APGARs were 4/4/9 at 1/5/10 minutes, respectively, and the neonate was subsequently transferred to the neonatal intensive care unit for respiratory distress where he required positive pressure ventilation, CPAP and supplemental oxygen. The infant went on to have a complicated course due to his large PDA, pulmonary hypertension, biventricular cardiac hypertrophy, intestinal malrotation requiring surgical intervention, and megacystis. The infant ultimately succumbed to respiratory failure. At autopsy, gross examination revealed an enlarged urinary bladder with an abnormally thick wall, normal liver, firm and darkly discolored lungs, and an enlarged heart. The ductus arteriosus was fully patent and approximately the same diameter as the aorta pulmonary trunk.

Patient 2 is a baby girl with a *de novo* *ACTA2* p.Arg179His mutation who had a complicated neonatal course that included surgical repair of a PDA and APW,

persistent pulmonary hypertension of the newborn that resolved 10 days after PDA surgery, and seizures and suspected moyamoya disease. She was subsequently diagnosed with congenital mydriasis, nephrolithiasis, and gastroesophageal reflux disorder. Genetic testing revealed the ACTA2 variant. At 22 months of age, she was admitted for acutely increased work of breathing in the setting of a possible viral illness. She died on hospital day 12 of her admission following attempted intubation for persistent tachypnea, increased work of breathing and carbon dioxide retention despite the use of Bilevel Positive Airway Pressure (BiPap).

On autopsy, gross examination revealed a flaccid-appearing urinary bladder with a thin wall. The pulmonary trunk was slightly enlarged and there was a small aneurysm on the posterior aspect of the proximal aorta. There was hyperinflation of the lung apices bilaterally with a wedge-shaped hemorrhagic area in the upper lobe of the right lung. The middle and lower lobes of the right lung were edematous with dark purple parenchyma and a firm, boggy consistency. The left lung was partially collapsed with the remainder of the lung pink and edematous with patchy firm areas. The lung parenchyma had multiple areas of microcystic architecture and extensive bronchiectasis. The liver was normal in appearance.

Patient 3 is a 32-year-old female with a *de novo* ACTA2 p.Arg179His mutation. Her past medical history, hospital course, and cerebrovascular pathology have been described previously (Georgescu et al., 2015). Briefly, she had a medical history of surgical repair of a PDA and thoracoabdominal aortic aneurysm, congenital absence of the iris, congenital intestinal malrotation, postural orthostatic

tachycardia, asthma, and dysrhythmia. She died secondary to large bilateral anterior cerebral artery and left middle cerebral artery infarcts resulting in herniation.

SMDS Associated Liver Pathology

Liver sections from the SMDS patients showed abnormalities in the portal triad not present in the livers of age matched controls who died of other causes. All three SMDS patients had expansion of the portal tracts with increased connective tissue deposition (**Figure 2.1a, c, asterisks**). In addition, the terminal branches of the hepatic artery in all three SMDS patients showed marked medial thickening in the affected patients when compared to controls (**Figure 2.1a, arrows**). The quantification of the thickness of the terminal branches of the hepatic artery in the SMDS patients' liver sections showed significant increase in the wall thickness when compared with control livers (**Figure 2.1b, d**).

All three patients were also noted to have additional abnormalities in the liver parenchyma suggestive of an overall poor metabolic state, including non-alcoholic hepatic steatosis in all three patients. The six-month old was noted to have intrasinusoidal nucleated erythrocytes, suggesting chronic hypoxia, likely secondary to this infant's longstanding severe pulmonary hypertension and resulting respiratory failure (Vazquez et al., 2015). Note, the infant control had sickle cell anemia also has intrasinusoidal nucleated erythrocytes potentially secondary to bone marrow necrosis (**Figure 2.1e, f**).

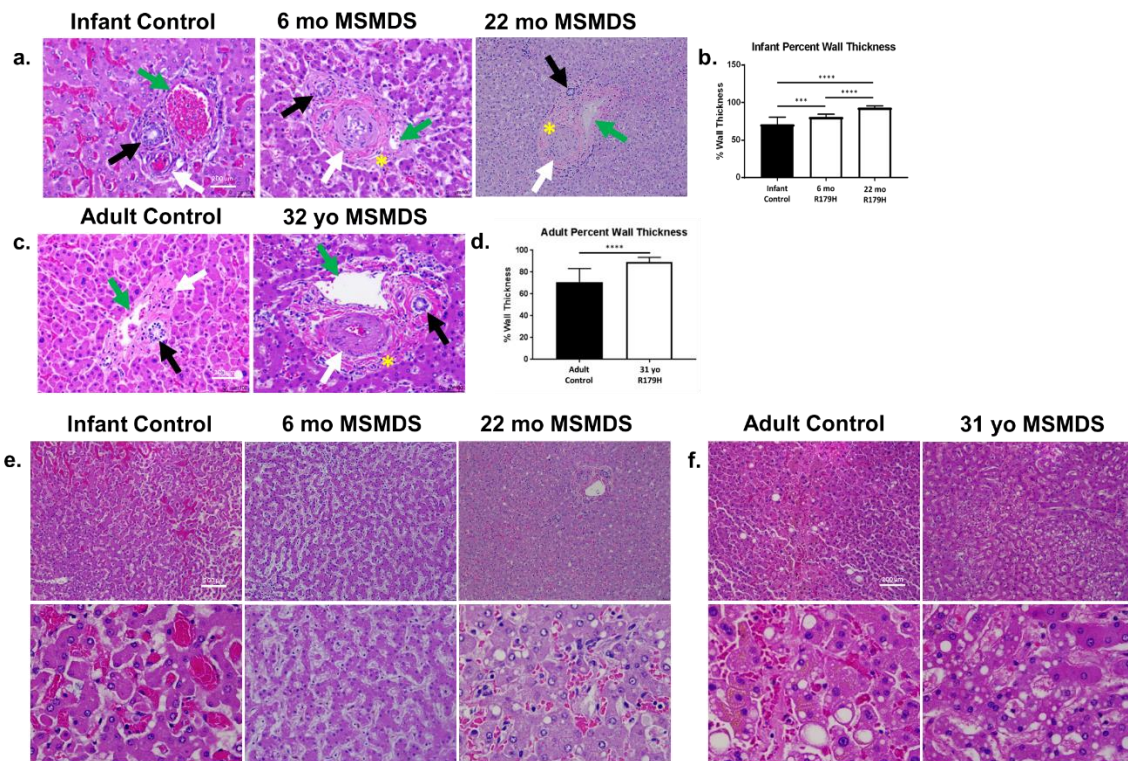


Figure 2.1. Thickening of the terminal branches of the hepatic artery, expansion of the portal tracts, and non-alcoholic hepatic steatosis in 6- and 22-month-old infants and a 32-year-old adult with SMDS. Hematoxylin and eosin staining of liver sections from all three patients with SMDS show thickening of the terminal branches of the hepatic artery compared to controls (**a, c, white arrow**). Quantification of the vessel wall thickness (percent) shows a significant increase in the artery wall thickness in both the 6 month ($p=0.0004$) and 22 month ($p\leq 0.0001$) old infants (**b**) and the 32 year ($p\leq 0.0001$) old adult (**d**) patients compared to the infant and adult control, respectively. Expansion of the portal tracts due to extracellular matrix deposition is also apparent in the SMDS patient tissue compared to the control (**a, c, asterisks**). The remainder of the portal triad, the portal vein (**a, c, green arrow**) and bile duct (**a, c, black arrow**), are normal in appearance. Finally, imaging of the liver parenchyma shows evidence of non-alcoholic hepatic steatosis in all three SMDS patients (**e**).

Lung Pathology in SMDS

All three patients had emphysematous changes and the two infant patients had evidence of pulmonary hypertension, similar to a previously reported patient with SMDS (**Figure 2.2**) (Milewicz et al., 2010b). The 6-month-old patient, who did not

undergo repair of his PDA, had advanced grade 2-3 pulmonary hypertension, with concentric, fibrocellular medial and intimal thickening of the pulmonary arterioles and small arteries with severe congestion (**Figure 2.2e, black arrowhead**). The 22-month-old patient, whose APW was repaired, had grade 1, pulmonary hypertension with hypertrophy of the media alone (**Figure 2.2e, white arrowhead**). Patient 3 did not have significant pulmonary arterial changes.

The alveolar spaces were significantly enlarged in all three patients, with the 31-year-old patient displaying the most severe emphysematous changes, including prominent interalveolar connections, pores of Kohn (**Figure 2.2d, black arrowheads**). Additionally, all three patients had significant thickening of the alveolar septae with congestion of the alveolar capillaries, most significantly in patient 1 (**Figure 2.2e, f, black arrows**).

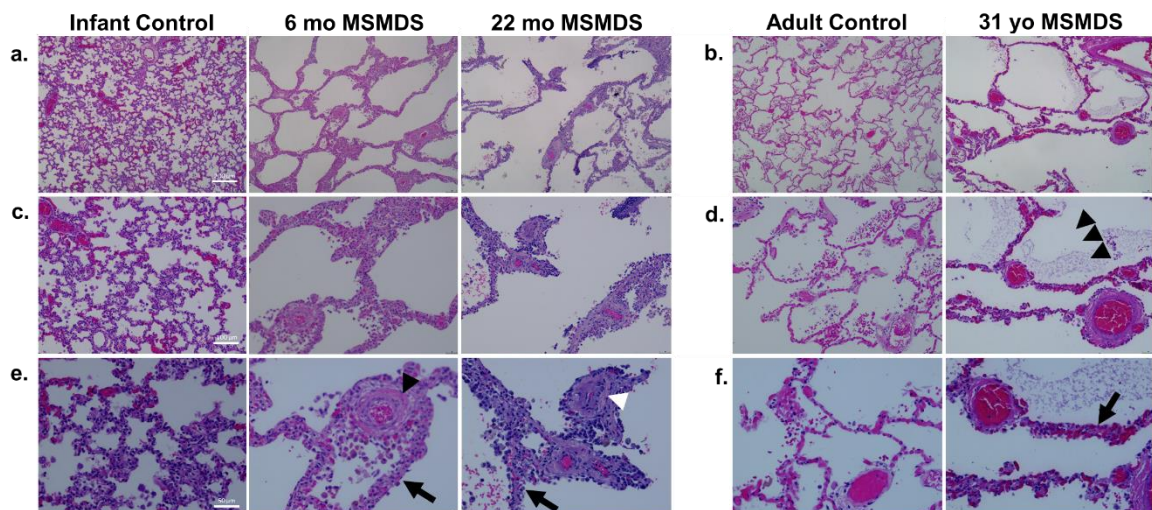


Figure 2.2. All three SMDS patients exhibit severe lung changes consistent with pulmonary hypertension and emphysematous changes. Hematoxylin and eosin staining demonstrated significant arterial wall thickening consistent with severe pulmonary hypertension. The 6-month old patient demonstrates advanced grade 2-3 pulmonary hypertension, with concentric, fibrocellular medial and intimal thickening of the pulmonary arterioles and small arteries with severe congestion (**e, black arrowhead**). The 22-month-old patient, whose APW was repaired, appeared to have less severe, grade 1, pulmonary hypertension with hypertrophy of the media alone (**e, white arrowhead**). In addition, all three patients had significant thickening of the alveolar septae with congestion of the alveolar capillaries (**e, f, black arrows**). Finally, alveolar spaces are significantly enlarged in all three patients with the 31-year-old patient displaying the most severe emphysematous changes, including prominent pores of Kohn (**d, black arrowheads**).

Discussion

We describe here pulmonary and hepatic pathology observed at autopsy in three patients with SMDS. The lung parenchyma of all three patients showed emphysematous changes, as was described in two previous patients (Regalado et al., 2018). Chronic lung disease and asthma requiring medication and even supplemental oxygen are frequent findings in patients with SMDS (Regalado et al., 2018). Hyperinflation of the upper lung segment and cystic lung disease have also been described in two patients (Milewicz et al., 2010b). The more detailed findings reported here, especially the emphysematous changes in the 6-month-old, suggest that SMDS causes selective defects in lung development.

Smooth muscle α -actin is expressed in both airway and vascular smooth muscle cells in the developing lung (Moiseenko et al., 2017). The lung develops in multiple stages starting with the embryonic stage, followed by the pseudoglandular, canalicular, saccular and finally the alveolar stage (Mullasery and Smith, 2015). Smooth muscle cell localization and regulation is crucial for the proper development of the lung (Danopoulos et al., 2018). Segmental branching of the airway occurs

early during the embryonic stage of lung development. Smooth muscle α -actin expressing cells play a central role in driving branching morphogenesis (Danopoulos et al., 2018; Goodwin et al., 2019). Disruption of smooth muscle cells during branching prevents terminal bifurcation during lung development interfering with alveolar formation (Kim et al., 2015). Studies in rodent models show that ASMA-expressing lung myofibroblasts participate in alveolar maturation, presumably guiding active septation (Dickie et al., 2007). In the normal lung, the pores of Kohn in the alveolar walls are small, but as the wall breaks down in destructive emphysema, the pores of Kohn enlarge and increase in number (Yoshikawa et al., 2016). This increase in the pores of Kohn, such as seen in these patients with SMDS, leads to a reduction in the area for gas exchange and a decrease in both the capillary bed and elastic recoil affecting pulmonary function (Yoshikawa et al., 2016). Taken together, alterations in SMA expressing lung smooth muscle cells and myofibroblasts caused by SMDS appears to impair alveolar development and enables airspace deterioration.

All three patients presented here had arterial changes consistent with pulmonary hypertension, an established complication of SMDS (Milewicz et al., 2010b; Regalado et al., 2018). SMDS also predisposes to moyamoya disease and pathologic changes of medial thickening and diffuse neointimal changes in the cerebrovascular arteries (Georgescu et al., 2015). Combined with our demonstration of arterial thickening in the liver outlined here, these findings suggest that SMDS leads to diffuse SMC arterial thickening. Fetal echocardiography of Patient 1 at 32 6/7 weeks found normal heart systolic function but mild dilatation of the main

pulmonary artery and ascending aorta, suggesting that pulmonary arterial changes are developmental in origin, independent of blood flow. Overall these observations suggest that the pulmonary arterial changes in patients with SMDS align with the pathology found in other muscular arteries in SMDS patients (Milewicz et al., 2010b; Munot et al., 2012; Georgescu et al., 2015).

Expansion of the portal tracts with increased connective tissue, medial thickening of the terminal branches of the hepatic artery, and non-alcoholic hepatic steatosis were noted in all three SMDS patients. Hepatic steatosis, an excessive accumulation of triglycerides within hepatocytes, has a wide range of etiologies, including alcoholic liver disease, drugs, disordered metabolism, and infections (Idilman et al., 2016). Given the health status of the three patients described here, metabolic causes of steatosis are plausible in these patients. One reason for why some patients with SMDS may go on to develop elevated liver enzymes and even fulminant liver failure is suggested by Graaff et al, 2018. They posit that relative hepatic hypoxia predisposes to progression of non-alcoholic fatty liver disease (van der Graaff et al., 2019). It is possible that the pulmonary pathology in conjunction with the significant thickening of the terminal branches of the hepatic artery in these SMDS patients may predispose these individuals to hepatic hypoxia and progressive liver disease. Hypoxia in turn can activate the resident hepatic macrophages, Kupffer cells (van der Graaff et al., 2019). Therefore, elevated transaminases and progression to fulminant liver failure in patients with SMDS may arise due to relative hypoxia leading to an inflammatory response by Kupffer cells, which in turn activate hepatic stellate cells (HSCs) through the secretion of TGF- β 1. Hepatic stellate cells

express high levels of SMA (Khomich et al., 2019). Hepatic steatosis alone can trigger HSC activation in the absence of other inflammatory processes due to increased TGF- β production by hepatocytes (Khomich et al., 2019). SMA in HSCs plays a critical role in contraction and cytoskeletal structure without significantly influencing proliferation or migration (Rockey et al., 2019). After carbon tetrachloride induced liver injury, *Acta2*^{-/-} mice expressed significantly fewer HSCs compared to *Acta2*^{+/+} mice with a corresponding reduction in collagen (Rockey et al., 2019). These findings suggest that SMA expression by HSCs plays a key role in liver wound healing and hepatic fibrosis (Rockey et al., 2019). By this view, mutations in *ACTA2*, such as the R179H mutation, would compromise hepatic repair and regeneration in response to injury.

In conclusion, patients with SMDS have a widespread arteriopathy, including narrowing of the intracranial arteries, aortic aneurysms and dissections, thickening of the terminal branches of the hepatic artery, and thickening of the pulmonary vasculature with pulmonary hypertension. Pathologically this arteriopathy is characterized by medial thickening. We recommend that patients with SMDS be monitored for liver disease and consider minimizing exposure to alcohol and medications metabolized in the liver. In addition, patients with SMDS should also be monitored closely for pulmonary complications and avoid risk factors that may augment the pulmonary disease.

Chapter Three: Smooth muscle cell specific knock-out of *Pcnt* leads to phenotypic modulation *in vitro* and atherosclerosis *in vivo*

Introduction

Majewski (or Microcephalic) Osteodysplastic Primordial Dwarfism Type II (MOPDII) is a rare autosomal recessive disorder due to biallelic loss of function mutations in the gene encoding the centrosome protein pericentrin, *PCNT* (Bober and Jackson, 2017). MOPDII is the most common form of microcephalic primordial dwarfism (Bober and Jackson, 2017). Patients with MOPDII have a very distinct clinical phenotype, including proportionate pre- and post-natal growth restriction with microcephaly, normal to near-normal intelligence, characteristic facial features, and bone dysplasia (Hall et al., 2004).

Unlike other forms of primordial dwarfism, vascular pathology is a leading cause of morbidity and mortality in these patients (Galasso et al., 2008; Bober and Jackson, 2017). Up to half of patients with MOPDII develop cerebrovascular pathology, including Moyamoya Disease and/or cerebral aneurysms (Bober et al., 2010). These patients also develop other diverse vascular pathology, including early-onset coronary artery disease, bicuspid aortic valve, atrial septal defect, patent ductus arteriosus, renal artery stenosis, and pulmonary artery stenosis (Bober and Jackson, 2017). With this in mind our laboratory created a smooth muscle cell specific *Pcnt* knock-out mouse to better understand the pathogenesis of the vascular phenotype in MOPDII. We can apply what we learn from rare conditions like MOPDII, which have a disproportionate incidence of early onset vascular disease, to better understand and treat more common forms of vascular disease as well.

Pericentrin

Pericentrin is a large coiled-coil protein, 380 kDa in humans and 360 kDa in mice, located on chromosome 21 in humans and chromosome 10 in mice (Mühlhans and Gießl, 2012). Pericentrin is a scaffold protein for the pericentriolar material, the collection of proteins making up the centrosome which is the main microtubule organizing center of the cell (Zimmerman et al., 2004). Through its role as a centrosome scaffold protein, pericentrin is involved in multiple cell functions, including microtubule nucleation, mitotic spindle orientation, and cell cycle regulation (Delaval and Doxsey, 2010).

During cell division the positioning of the mitotic spindle determines if a cell divides symmetrically into two identical daughter cells or asymmetrically into two daughter cells destined for different cell fates (Alberts et al., 2015). In the absence of pericentrin, neural progenitor cells undergo symmetric cell division at a lower than normal rate potentially leading to the microcephaly seen in patients with MOPDII (Delaval and Doxsey, 2010; Chen et al., 2014a). Pericentrin plays a pivotal role in centrosome microtubule nucleation by anchoring the γ -Tubulin Ring Complex (Zimmerman et al., 2004; Alberts et al., 2015). Microtubules may originate either from the centrosome, radial microtubules, or from sites outside the centrosome such as the Golgi, directional microtubules (O'Rourke et al., 2014). Pericentrin works in an antagonistic manner with another protein, Cep192, to regulate microtubule nucleation (O'Rourke et al., 2014). Depletion of pericentrin offsets this balance leading to an increase in centrosome microtubule nucleation and may affect cell migration (O'Rourke et al., 2014). Finally, pericentrin has been shown to play a direct role in cell cycle regulation through the ataxia telangiectasia and rad3 related

(ATR) pathway where it anchors checkpoint kinase 1 (Chk1) to the centrosome (figure 3.1) (Griffith et al., 2008; Tibelius et al., 2009; Delaval and Doxsey, 2010). When localized to the centrosome, Chk1 inhibits G2/M cell cycle progression through inactivation of Cdc25B (Schmitt et al., 2007; Tibelius et al., 2009). In turn, knock down of pericentrin in U2OS cells has been shown to lead to an increase in cells in late G2 and mitosis (Tibelius et al., 2009).

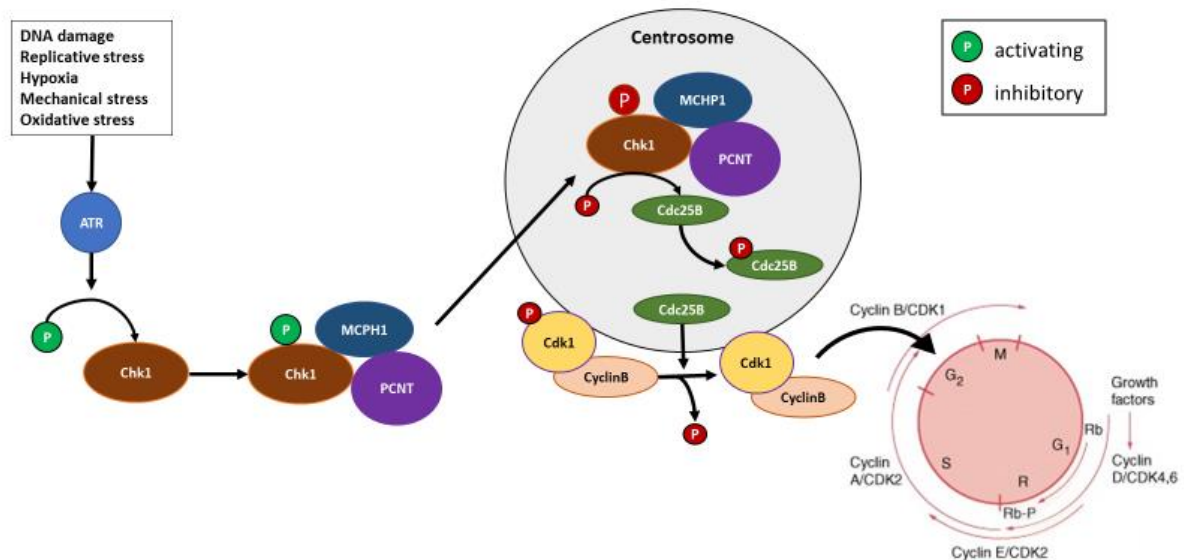


Figure 3.1. Role of pericentrin in the ATR-Chk1 pathway. Various stimuli, including mechanical stress, hypoxia, and oxidative stress, activate ATR leading to the phosphorylation of Chk1. p-Chk1 is then recruited to the centrosome by microcephalin (MCPH1) and pericentrin (PCNT). Once at the centrosome, p-Chk1 phosphorylates Cdc25B, deactivating it. This in turn leads to a reduction in Cdc25B-mediated dephosphorylation of p-Cdk1/CyclinB and inhibition of G2/M cell cycle progression.

Vascular Smooth Muscle Cells in Atherosclerosis

Vascular smooth muscle cells are the main cell type making up the artery wall, localized to the medial layer where they contract to regulate blood pressure and

produce extracellular matrix (El-Hamamsy and Yacoub, 2009). Differentiated smooth muscle cells express an array of contractile proteins, including α -smooth muscle actin (SMA), smooth muscle myosin heavy chain (SMMHC), calponin, and smooth muscle 22 α (SM22 α) (Frismantiene et al., 2018). Unlike other muscle cells, vascular smooth muscle cells have the ability to de-differentiate in response to certain environmental stimuli, from a non-proliferative and non-migratory contractile phenotype to a proliferative and migratory synthetic phenotype (Owens et al., 2004; El-Hamamsy and Yacoub, 2009). In the pre-atherosclerotic stage, vascular smooth muscle cells migrate from the medial layer of the cell to the intimal layer where they produce proteoglycans and elastin leading to diffuse intimal thickening (Dubland and Francis, 2016). In the early stages of atherosclerotic disease development, extracellular LDL deposits form a fatty streak in the deep intimal layer (Dubland and Francis, 2016). Once within the intimal layer SMCs de-differentiate from a contractile phenotype to a proliferative, synthetic phenotype (Dubland and Francis, 2016). Thickness of the fibrous cap overlying atherosclerotic plaques is associated with plaque stability with a thin cap and a high ratio of macrophages to SMCs being associated with an unstable plaque (Shankman et al., 2015).

Foam cells were originally thought to be derived exclusively from macrophages containing intracellular lipid droplets (Rong et al., 2003). Studies have shown that loading of SMCs with cholesterol can induce the downregulation of contractile markers, including SMA, α -tropomyosin, SMMHC, and calponin H1, and upregulation of macrophage markers, including CD-68 and Mac-2 (Rong et al.,

2003). This change was found to occur rapidly, within 48 to 72 hours (Rong et al., 2003). Rong et al suggests that this process is a transdifferentiation process, rather than de-differentiation. Lineage tracing experiments labeling SMCs have further shown that as much as 82% of SMCs within atherosclerotic lesions are *ACTA2* negative on immunostaining and transdifferentiated, or phenotypically modulated, SMCs comprised as much as 30% of macrophage-like cells within atherosclerotic lesions (Shankman et al., 2015). The downregulation of smooth muscle cell markers in phenotypically modulated SMCs was further shown to be due to suppression by Kruppel-like Factor 4 (KLF4) (Shankman et al., 2015). Recently, using single cell RNA-Sequencing (scRNA-Seq), Wirka et al identified a distinct subset of phenotypically modulated SMCs that appear and increase with disease progression in atherosclerotic plaques in *Apoe*^{-/-} (apolipoprotein E) mice fed a high fat diet (HFD) (Wirka et al., 2019). These modulated SMCs (mSMCs) reduce expression of contractile markers and upregulate expression of markers of macrophage, fibroblasts (like *Spp1* and *Fn1*) and stem cells (*Sca1*).

Several intracellular and extracellular factors can induce endoplasmic reticulum (ER) stress and a consequent unfolded protein response (UPR). The UPR becomes activated when the folding capacity of the ER is overwhelmed by the accumulation of unfolded or misfolded proteins, in addition to the increased expression of normal proteins, nutrient deprivation, alterations in calcium homeostasis, or oxidative stress (Chattopadhyay et al., 2020). Inflammatory and vascular cells within atherosclerotic lesions have been shown to have chronic ER stress leading to activation of the UPR (Zhou et al., 2015). Stimulation of the UPR

leads to the activation of three pathways: the protein kinase RNA-like ER kinase (PERK) pathway, the inositol-requiring enzyme-1 (IRE1 α) pathway, and the activating transcription factor 6 (ATF6) pathway (Bravo et al., 2013). Upon accumulation of unfolded proteins, BiP/GRP78 dissociate from PERK leading to its activation (Bravo et al., 2013). Once activated, the PERK pathway phosphorylates the alpha subunit of the eukaryotic translation initiation factor-2 (eIF2- α) which in turn activates ATF4 with downstream activation of C/EBP homologous protein (CHOP) among other factors (Bravo et al., 2013). Chronic activation of CHOP may then lead to apoptosis (Zhou et al., 2015). IRE1 α in turn must dissociate from BiP/GRP78 and directly interact with unfolded proteins to be activated (Bravo et al., 2013). Once activated IRE1 α catalyzes splicing of the X-box-binding protein-1 (*XBP1*) mRNA, which then activates several genes including ER degradation enhancing α -mannosidase like protein 1 (EDEM) and other genes involved in ER protein synthesis, vesicular trafficking, lipid biogenesis, and autophagy (Bravo et al., 2013). Finally, ATF6 is normally retained in the ER through activation with BiP/GRP78 and calreticulin, but during ER stress is transported to the Golgi apparatus on vesicles where it is cleaved (Bravo et al., 2013). The N-terminal fragment is then translocated to the nucleus where it promotes transcription of UPR genes such as the transcription factors XBP1 and CHOP, and the chaperones GRP94 and BiP/GRP78 (Bravo et al., 2013).

Kruppel-like factor 4 (KLF4) is a one of a group of proteins, also including OCT4, SOX2, and c-MYC, which together enable the re-programming of terminally differentiated cells into pluripotent stem cells (Schuetz et al., 2011). KLF4 is a zinc-

finger transcription factor belonging to the Sp/Klf family (Schuetz et al., 2011). In SMCs, KLF4 acts through two key mechanisms: binding to the G/C repressor element in several SMC contractile genes, including *ACTA2*, *TAGLN* and *MYH11*, and inhibiting binding of SRF to CArG elements, to downregulate the expression of SMC contractile genes (Shankman et al., 2015). Activation of KLF4 is tied to the PERK pathway through ATF4, which has been shown to both promote transcription of *KLF4* and suppress the proteasomal degradation of KLF4 (Zhou et al., 2015). Recent data from our lab have shown that cholesterol treatment activates the UPR and this UPR drives cholesterol-induced phenotypic modulation of SMCs to proatherogenic modulated SMCs, primarily through the PERK arm of UPR (Chattopadhyay et al., 2020). Upregulation of macrophage-specific markers and a large subset of fibroblast-specific markers was inhibited by co-treatment with both 4-phenylbutyric acid (4-PBA), a general inhibitor of ER stress, and integrated stress response inhibitor (ISRIB), a specific inhibitor of PERK signaling (Chattopadhyay et al., 2020).

Unpublished data from our lab have demonstrated that cholesterol treatment activates not only ER stress, but also cytosolic stress in SMCs. Cytosolic stress or the heat shock response involves the activation of heat shock proteins (HSPs) to mediate the refolding or degradation of damaged proteins, primarily by the transcription factor heat shock factor 1 (HSF1) (Barna et al., 2018). When activated, HSF1 becomes trimerized and phosphorylated before translocating to the nucleus where it binds to conserved heat shock-responsive DNA elements (HSEs) (Barna et al., 2018). HSF1 is regulated via a negative feedback loop through which several of

the proteins it activates, including HSP70, HSP72, and HSP90, directly inhibit HSF1 through binding to its trimerization domain (Barna et al., 2018). The HSP chaperone family have diverse roles in cellular function: HSP90 binds damaged proteins and directs them to HSP60 and HSP70 for further processing, in addition to playing diverse roles in signal transduction systems (Barna et al., 2018).

In addition to its role in heat shock response, HSP70 is also required for the proper assembly of pericentriolar material (PCM) (Fang et al., 2019). PCM contains hundreds of proteins including microtubule nucleating factors, signaling molecules and cell cycle regulators in addition to the scaffold protein pericentrin (Fang et al., 2019). Errors in the proper accumulation of PCM at the centrosome can lead to a functionally compromised mitotic centrosome with multipolar or disorganized spindles leading to mitotic arrest, aneuploidy and/or cell death (Fang et al., 2019). HSP70 is phosphorylated by NEK6 targeting HSP70 to the mitotic spindle where it cooperates with PCNT and CEP215, among other proteins, to ensure their proper assembly at the mitotic centrosome (Fang et al., 2019).

Here we describe unique coronary artery pathology from two patients with MOPDII. We go on to utilize a novel smooth muscle cell specific pericentrin knock-out mouse to investigate the role of the ATR pathway and phenotypic modulation in disease development. We show that *Pcnt*^{SMKO} cells display activation of UPR and cytosolic stress pathways associated with phenotypic modulation and atherosclerotic phenotype *in vivo*.

Materials and Methods

Patient Tissue

The study protocol was approved by the Institutional Review Board of the University of Texas Health Science Center at Houston and the patient or family members consented to these studies. Coronary artery tissue was obtained at autopsy and stained with hematoxylin and eosin (H&E) and Movat pentachrome stain, and immunostained with anti-SMA (Sigma 5228) and anti-CD68 antibodies.

Mouse Generation

All mouse experiments were carried out in accordance with institutional guidelines at The University of Texas at Houston for the care and use of animals. Embryonic stem cell clones in a C57BL/6 background with the targeted *Pcnt* allele (EPD0724_5_F03, B04 and A03) were purchased from the European Conditional Mouse Mutagenesis program (EUCOMM.org). The targeting vector was designed to contain a 5391 bp 5' targeting arm, a *LacZ* and a *neo* expression cassette which were flanked by two Frt sites. In addition, it contained a 1499 bp mouse *Pcnt* fragment (spanning exons 17 and 18) that were flanked by two loxP sites and a 4438 bp 3' targeting arm allowing for Cre-mediated conditional deletion of the *Pcnt* gene between exons 17 and 18 leading to an out-of-coding frame shift, generating a premature stop codon and a loss-of-function allele (figure 3.2). The embryonic stem cell clones were microinjected into C57BL/6 blastocysts. Male chimeric founder mice were bred with albino C57BL/6 females. Male chimeric mice with proven germ line transmission then bred into 129 SvEv FLPeR mice (stock #003946, Jackson Lab) to remove the Frt-flanked *LacZ* and *neo* cassettes. The $Pcnt^{fl/fl}$ were then crossed into SMA-Cre-ERT2 mice in a 129SvEv background. Resulting $Pcnt^{fl/+}$, SMA-Cre-ERT2^{+/-} mice were crossed with $Pcnt^{fl/+}$ mice to produce $Pcnt^{fl/fl}$, SMA-Cre-ERT2 mice. For

experiments, $Pcnt^{fl/fl}$, SMA-Cre-ERT2^{+/-} males were crossed with $Pcnt^{fl/fl}$ females to produce a Mendelian ratio of 50% $Pcnt^{fl/fl}$, SMA-Cre-ERT2^{+/-} and 50% $Pcnt^{fl/fl}$ to use as littermate controls.

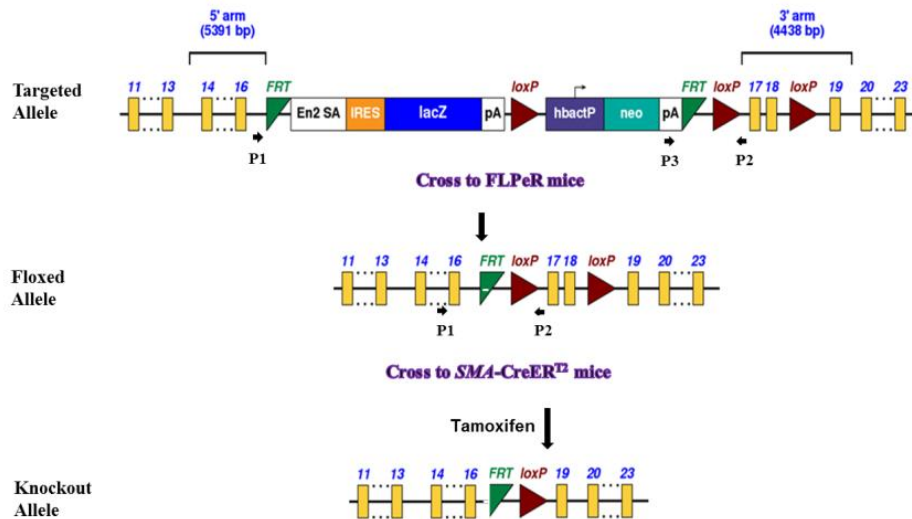


Figure 3.2. Pcmt-flox mouse construct and resulting cross into SMA-CreERT² mice.

Smooth muscle cell explant and cell culture conditions and cholesterol exposure

Ascending and descending aortic smooth muscle cells were isolated from 6-8 week old $Pcnt^{fl/fl}$, SMA-Cre-ERT2^{+/-} mice according to previously published methods (Kwartler et al., 2016). In brief, 3-6 mice per an experiment were anesthetized with an IP injection of 2.5% avertin. Once the mouse was sufficiently anesthetized, the thorax was exposed, the lungs removed to expose the aorta and its branches. Microdissection technique was then used to dissect out and clean the heart, aorta and aortic branches. Further cleaning was done in DPBS under a dissecting microscope to remove any fatty or connective tissue. Once sufficiently cleaned, the ascending aorta including the carotid arteries were separated from the descending aorta using a scalpel and placed in separate labelled containers in aorta biopsy

storage media. Aortic and carotid artery tissue was isolated from 3-6 mice in this manner, combining the ascending and descending aortic tissue from all mice into their respective dishes.

Once all the tissue had been thoroughly cleaned, digestion media was prepared, the tissue washed in ethanol briefly and then rinsed in PBS. The tissue was cut into fragments for digestion and allowed to digest overnight. Once tissue was digested with visible floating cells, tissue and cells were spun down and transferred to a new 10 cm dish in smooth muscle basal medium (Promo Cell) supplemented with 20% fetal bovine serum (FBS, Gibco), insulin, epidermal growth factor, fibroblast growth factor (Promo Cell), HEPES (Millipore Sigma), sodium pyruvate (Millipore Sigma), L-glutamine (Millipore Sigma), and antibiotic/anti-mycotic (Millipore Sigma).

Free cholesterol complexed to methyl- β -cyclodextrin (MBD-Chol), containing ~40mg cholesterol per gram of product, was purchased from Millipore Sigma and dissolved in deionized water. All calculations for cholesterol treatment were based on the weight of cholesterol in the MBD-Chol complex. Explanted SMCs were treated with 0, 2.5, and 10 μ g/mL MBD-Chol (as described by Rong and colleagues) in Dulbecco's Modified Eagle Medium (DMEM) containing high glucose (Cellgro), 10% FBS (Gibco), 1% antibiotic/anti-mycotic (Millipore Sigma) and 0.2% bovine serum albumin (BSA, Fisher Scientific) for 72 hours at 37C and 5% CO₂.

Protein extraction and Western blot

For protein analysis, when cultured cells were confluent, cold lysis buffer was prepared (50mM Tris-HCl pH 7.5, 150mM NaCl, 1% Triton X-100 and 1mM EDTA)

with protease inhibitor cocktail (Millipore Sigma) and phosphatase inhibitor cocktails (Millipore Sigma). Cells were collected via scraping and incubated in lysis buffer for 15 minutes followed by 15 second sonication. Crude lysates were then cleared via centrifugation at top speed for 10 minutes at 4 C. Bradford was performed per protocol (BioRad Laboratories) and protein concentrations quantified. For pericentrin 60-80 µg of protein was resolved on a 4% gel (ProtoGel National Diagnostics). For all other samples 10-30 µg of protein was resolved on 4-20% TGX gels (Bio-Rad Laboratories). Protein was then transferred to PVDF membranes (Millipore Sigma), blocked with 5% dry milk (or 5% BSA for detecting phosphorylated proteins, Atf4, and pericentrin) in Tris-buffered saline (TBS), containing 0.05% Tween-20 (TBST) and the membrane probed with different antibodies (Table 1). Bands were visualized by chemiluminescent substrate (GE Healthcare) on a BioRad Imager. Band intensities on the immunoblots were quantified using ImageJ software.

TABLE 3.1: List of antibodies used for Western blot

Target Antigen	Vendor/Source	Catalog #
α-smooth muscle actin (α-SMA)	Millipore Sigma	A5228
Atf4	Cell Signaling Technologies	11815S/D4B8
Atf6	ThermoFisher Scientific	NBP14025601
α-Tubulin (DM1A)	Cell Signaling Technologies	CST 3873T
Cdc2/Cdk1	Cell Signaling Technologies	CST 77055
Cdc25B	Cell Signaling Technologies	CST 9525
Cd68	Abcam	ab125212
Calponin (Cnn1)	Thermo Fisher Scientific	PIMA511620
Chk1	Cell Signaling Technologies	CST 2360S
eIF2α	Cell Signaling Technologies	5342S/D7D3

Gapdh	Cell Signaling Technologies	CST 14C10
Hsp70	Cell Signaling Technologies	CST 4872
Hsp90	Cell Signaling Technologies	CST 4874
Ire1 α	Abcam	ab37073
Klf4	RnD Systems	
Lgals3	Abcam	ab76245/EP2775Y
Pericentrin /Pericentrin-2	Abcam	ab4448
Phospho-Cdc2/Cdk1 (Tyr15)	Cell Signaling Technologies	CST 4539
Phospho-Cdc25B (Ser323)	Abcam	ab53103
Phospho-Chk1 (Ser345)	Cell Signaling Technologies	CST 2348
Phospho-eIF2 α	Cell Signaling Technologies	3398S/D9G8
Phospho-Ire1 α (phospho S724)	Abcam	ab48187
SM22- α /TAGLN/transgelin	Abcam	ab14106
Smooth Muscle Myosin Heavy Chain	Abcam	Ab53219

RNA extraction, quantitative real-time PCR (qPCR)

Total RNA was isolated from cultured SMC explants, quantified by Nanodrop (Thermo Fisher Scientific), and then used for cDNA synthesis using QScript reagent (Quantabio). mRNA expression for macrophage-specific and ER stress-specific genes was estimated using SYBR green chemistry (primers were obtained from Millipore Sigma and reaction master mix from Quantabio, Table 2) and for SMC contractile genes using Taqman probes (Taqman probes were purchased from Applied Biosystems and qPCR master mix obtained from Takara Biosciences). Reactions were performed in triplicate. 18S rRNA and Gapdh were used as endogenous controls for SYBR and Taqman reactions, respectively.

TABLE 3.2: List of SYBR primers used for quantitative real-time PCR (qPCR)

Gene	Forward primer (5' -> 3')	Reverse primer (5' -> 3')
------	---------------------------	---------------------------

<i>Cd68</i>	CAAGGTCCAGGGAGGTT GTG	CCAAAGGTAAGCTGTCC ATAAGGA
<i>Lgals3</i>	AGGAGAGGGAATGATGT TGCC	GGTTTGCCACTCTCAAAG GG
<i>Abca1</i>	GCGGACCTCCTGGGTGT T	CAAGAATCTCCGGGCTTT AGG
<i>Klf4</i>	CTGAACAGCAGGGACTG TCA	GTGTGGGTGGCTGTTCT TTT
Unspliced <i>Xbp1</i> (<i>uXbp1</i>)	CAGCACTCAGACTATGT GCA	GTCCATGGGAAGATGTT CTGG
Spliced <i>Xbp1</i> (<i>sXbp1</i>)	CTGAGTCCGAATCAGGT GCAG	GTCCATGGGAAGATGTT CTGG
<i>Atf4</i>	GGGTTCTGTCTTCCACTC CA	AAGCAGCAGAGTCAGGC TTTC
<i>Chop</i>	CCACCACACCTGAAAGC AGAA	AGGTGAAAGGCAGGGAC TCA
<i>Grp94</i>	AAGAATGAAGGAAAAACA GGACAAAA	CAAATGGAGAAGATTCC GCC
<i>BiP</i>	TTCAGCCAATTATCAGCA AACTCT	TTTTCTGATGTATCCTCT TCACCAGT
<i>Edem</i>	CTACCTGCGAAGAGGCC G	GTTTCATGAGCTGCCCAC TGA
<i>Hsf1</i>	GGACAGGAACAGCTCCT TGA	TCCTGTTTCCCCTTCATC AG
<i>Hsp70</i>	CAGCGAGGCTGACAAGA AGAA	GGAGATGACCTCCTGGC ACT
<i>Hsp90aa1</i>	AATGCTTAGAACTATTTA CTGAACTAGCAGAA	GTCCTCGTGAATTCCAAG CTTT
<i>Hsp90ab1</i>	GCGCACGCTGACTTTGG T	CCTGGAGAGCCTCCATG AAC
<i>Serping1</i>	GCCCAATTCGATGACCAT AC	AAGTTGGTGCTTTGGGA ACA
<i>Fn1</i>	CGAGGTGACAGAGACCA CAA	CTGGAGTCAAGCCAGAC ACA
<i>Ecr4</i> (1500015O10Rik)	AAGCGTGCCAAACGACA GCTGTGGGAC	TTAATAGTCATCATAGTT GACTGGC
<i>Fmod</i>	CAACACCAACCTGGAGA ATCTTT	GTGCAGAAGCTGCTGAT GGA
<i>Prg4</i>	GAAAATACTTCCCGTCTG CTTGT	ACTCCATGTAGTGCTGAC AGTTA
<i>Spp1</i>	TCACCATTTCGATGAGTC TG	ACTTGTGGCTCTGATGTT CC
<i>Lcn2</i>	TGCCACTCCATCTTTCCT GTT	GGGAGTGCTGGCCAAAT AAG
<i>Timp1</i>	CCAGAGCCGTCACCTTG CTT	AGGAAAAGTAGACAGTG TTCAGGCTT

<i>Bgn</i>	ATTGCCCTACCCAGAACT TGAC	GCAGAGTATGAACCCTTT CCTG
<i>Dcn</i>	TTCCTACTCGGCTGTGA GTC	AAGTTGAATGGCAGAAC GC

Immunofluorescent staining

Cover slips were irradiated and then plated with 10,000 to 20,000 cells each. Cells were allowed to adhere overnight and then treated with 10 ng/ml TGF- β 1 for 72 hours. Cells were washed in DPBS and fixed with 4% paraformaldehyde in 0.1M phosphate buffer for 20 minutes. Cells were permeabilized in 0.3% TritonX-100 in DPBS for 30 minutes and blocked in 2.5% BSA in DPBS plus 0.1% Tween20. Cells were incubated in primary antibody (see Table 1) at 4 C overnight followed by secondary antibody 1 hour at room temperature. Cells were incubated in 2.5% Texas-Red-Phalloidin (Thermo Fisher Scientific) stain per protocol for 30 minutes at room temperature. Coverslips were then mounted on slides using Vectashield with DAPI (Vector Laboratories). Slides were imaged using a Leica DMI8 confocal microscope.

BrdU incorporation cell proliferation assay

Assay performed per protocol (Cell Signaling Technologies). In brief, cells were seeded in 96-well plate, 5,000-10,000 cells per well. Cells were allowed to attach overnight then cells were serum starved for 24 hours followed by treatment with 5 ng/ml PDGF-BB for 24 hours. Cells were then treated with BrdU for 24 hours then fixed and incubated in primary and secondary antibodies per protocol. Substrate was incubated for 30 minutes at room temperature and then absorbance at 450 nm read.

Wound healing migration assay

Cells were plated in a 12 well plate in triplicate and allowed to become confluent. Once confluent, a wound was made using a 21G needle. The plate was then rinsed with DPBS and placed in serum free media. Brightfield images were captured on a Zoe Fluorescent Cell Imager (BioRad) at 175x magnification at 0 and 24 hours. Wound width was measured in ImageJ at three points per well and averaged, and the percent wound closure averaged over three wells.

Klf4 transactivation assay

A Klf4 transactivation assay was performed using a Cignal Reporter Plasmid (Qiagen) and the luciferase activity measured using a Dual Luciferase Reporter Assay Kit (Promega) per the manufacturer's instructions. In brief, 25,000 SMCs were plated in triplicate on 24-well plates and transfected with 250 ng Klf4 Cignal Reporter Plasmid (Qiagen) using Lipofectamine reagent (Life Technologies) for 4 hours. Cells were then treated with or without cholesterol for 72 hours. Following incubation, the cells were subjected to luciferase assay using a Dual Luciferase Reporter Assay Kit (Promega) according to manufacturer's instructions. Klf4 transcriptional activity was quantified as the ratio between the luminescence from firefly luciferase and Renilla luciferase.

Heat shock element luciferase assay

Heat shock element (HSE) luciferase assay was performed by transfecting 25000 SMCs (in triplicates) with 250ng HSE Cignal Reporter plasmid (Qiagen) using Lipofectamine reagent (Life Technologies), followed by treating the cells with cholesterol and finally measuring the firefly and Renilla luciferase luminescences

using a Dual Luciferase Assay Kit (Promega), as per manufacturer's instructions. HSE luciferase activity, a measure of Hsf1 binding to the HSE, was expressed as the ratio between the firefly and the Renilla luciferase luminescences.

Echocardiography

Echocardiography measurement (Vevo 3100 imaging system; MX550D, 40 MHz transducer; VisualSonics, Toronto, Canada) was performed 2 weeks post-operation (Zhou et al., 2019). Briefly, mice were weighed and anesthetized by 0.5 to 1.0 L/min room air with 2% isoflurane via nose cone. The heart rate was closely monitored and the body temperature was maintained around 38.5°C using the heating system. Mouse aortic root and ascending aorta were imaged in B-mode. Left ventricular function derived from short-axis parasternal planes was imaged using M-mode. Three measurements were taken of maximal internal diameter at the aortic root and ascending aorta. Left ventricular function measurements were gained from 3 different cardiac cycles and averaged. Data were analyzed by operator blinded to the treatment groups.

AAV-PCSK9^{DY} injection and Oil Red O Staining

Six-week-old mice were injected with 1.1×10^9 viral particles via retroorbital injection. They were allowed to recover for one week and then switched to a high fat diet (42% from fat, Envigo) for 14 weeks. At the end of 14 weeks mice were weighed, cholesterol measured, and blood collected. Mice were then sacrificed and the whole aorta, from aortic root to iliac bifurcation was collected and the outside thoroughly cleaned. The aorta was then opened and pinned en face and Oil Red O staining performed per protocol. Pictures were then taken and the images analyzed using

ImageJ. For image analysis, the whole aortic area was measured followed by the area of Oil Red O staining. The percent lesion was calculated by taking the lesion area and dividing by the total aortic area and multiplying by one-hundred.

Results

Atherosclerotic disease in patients with MOPDII

Coronary artery tissue was obtained from two siblings with MOPDII who both died of complications of vascular diseases. Patient 1 had a past medical history of kidney transplantation for chronic kidney disease, bilateral bypass revascularization for moyamoya disease, and clipping of a left vertebral artery aneurysm. He did have hypertension and hypercholesterolemia. Patient 1 suffered a lethal myocardial infarction and died at the age of 25 years.

Patient 2 was the sister of patient 1 who had MOPDII. She had a past medical history of stage IV chronic kidney disease, tracheomalacia status post tracheostomy, asthma, diastolic cardiac dysfunction, and multilevel coronary artery disease. During a paraesophageal hernia repair she suffered an acute ischemic stroke in addition to developing a klebsiella urinary tract infection leading to acute kidney disease requiring dialysis. This was further complicated by additional myocardial infarction, sepsis, and acute respiratory distress syndrome.

At autopsy, patient 1 was found to have severe stenotic coronary arteriopathy, with both the left and right coronary arteries showing variable degrees of fibromuscular intimal thickening and associated atheromatous changes. The proximal to mid right coronary artery had complete stenosis with superimposed thrombus. The proximal to mid left anterior descending coronary artery had marked

stenosis also with a superimposed thrombus. There were extensive areas of myocardial infarction involving both the left and right ventricle and the interventricular septum most prominent in the posterior and lateral walls of the left ventricle.

Histologic examination revealed large atheromatous plaques containing SMCs, calcification, and cholesterol crystals surrounded by macrophages, loss of cells in the medial layer and increased elastosis in the adventitial layer (figure 3.3).

Immunostaining of a SMC marker, smooth muscle α -actin, revealed increased numbers of positive staining cells in the adventitial layer but few vacuolated SMCs in the medial layer.

At autopsy, patient 2 was also found to have a stenotic coronary arteriopathy, with 90% occlusion of the right coronary artery, and 30% occlusion of the left main, left anterior descending and left circumflex coronary arteries. There was evidence of multiple prior myocardial infarctions involving the posterior-lateral left ventricle and posterior interventricular septum with patchy interstitial fibrosis throughout the right ventricle, posterior interventricular septum, and posterior-lateral left ventricle with associated myocyte hypertrophy. The aortic arch had numerous calcifications and the descending aorta showed medial calcification and intimal hyperplasia.

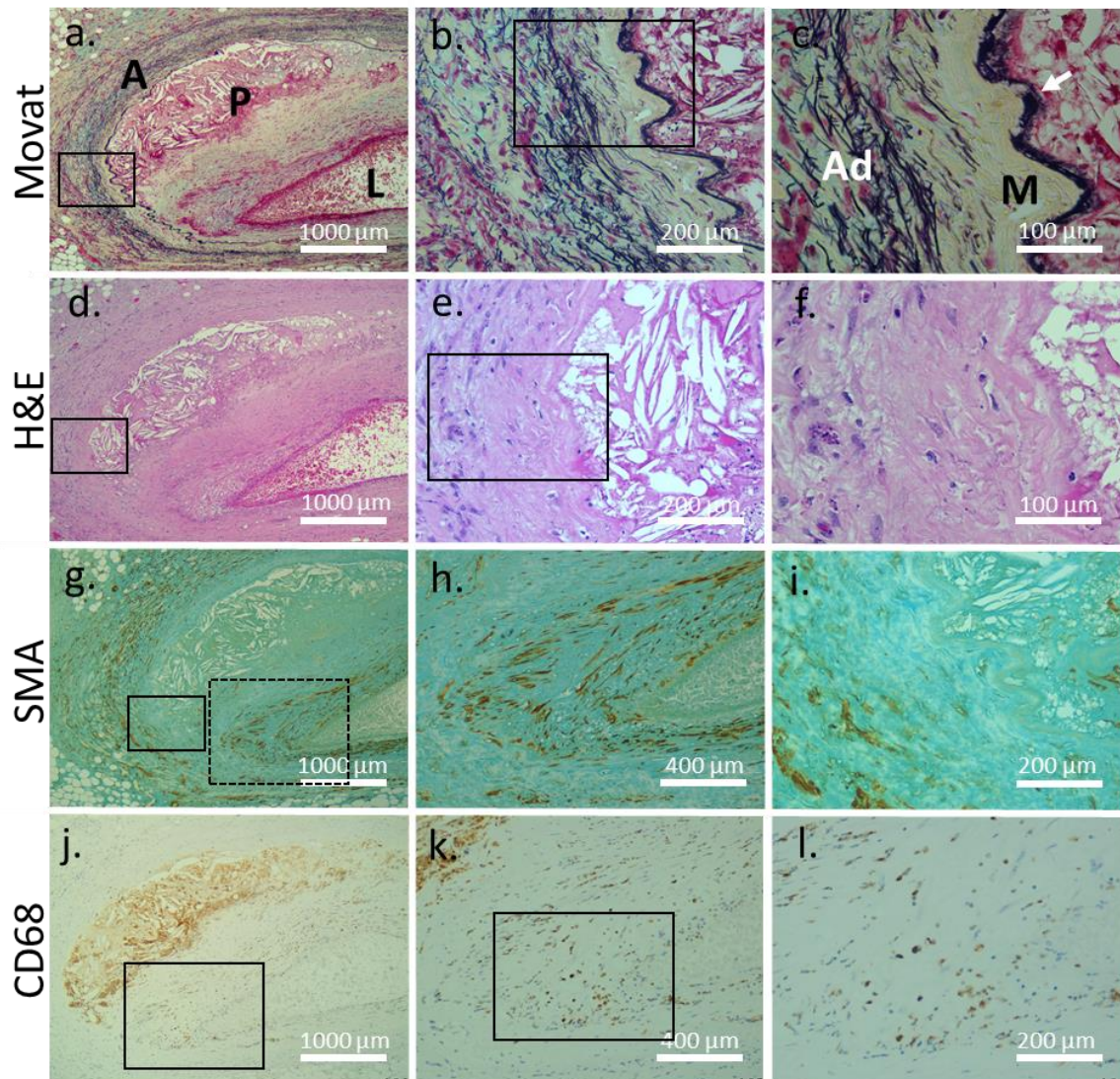


Figure 3.3. Left anterior descending coronary artery from MOPDII patient 1. Low magnification image of Movat staining (a) reveals a large atherosclerotic plaque (P) in the left anterior descending coronary artery with a small residual lumen (L). Higher magnification image (b, c) of the artery wall (A) shows a well-formed internal elastic lamina (c, arrow) with an absence of cell staining in the medial layer (M) and elastosis in the adventitial layer (Ad). Hematoxylin and eosin staining (d-f) shows these findings along with cholesterol crystals in the atherosclerotic plaque. Alpha-smooth muscle actin (SMA) staining reveals large numbers of SMA-positive cells in the adventitia and fibrous cap (g, h) of the atherosclerotic plaque, while confirming an absence of SMA-positive cells in the medial layer (i). Finally, staining for the macrophage marker CD68 reveals staining in the atherosclerotic plaque (j), and CD68-positive cells within the fibrous cap (k, l).

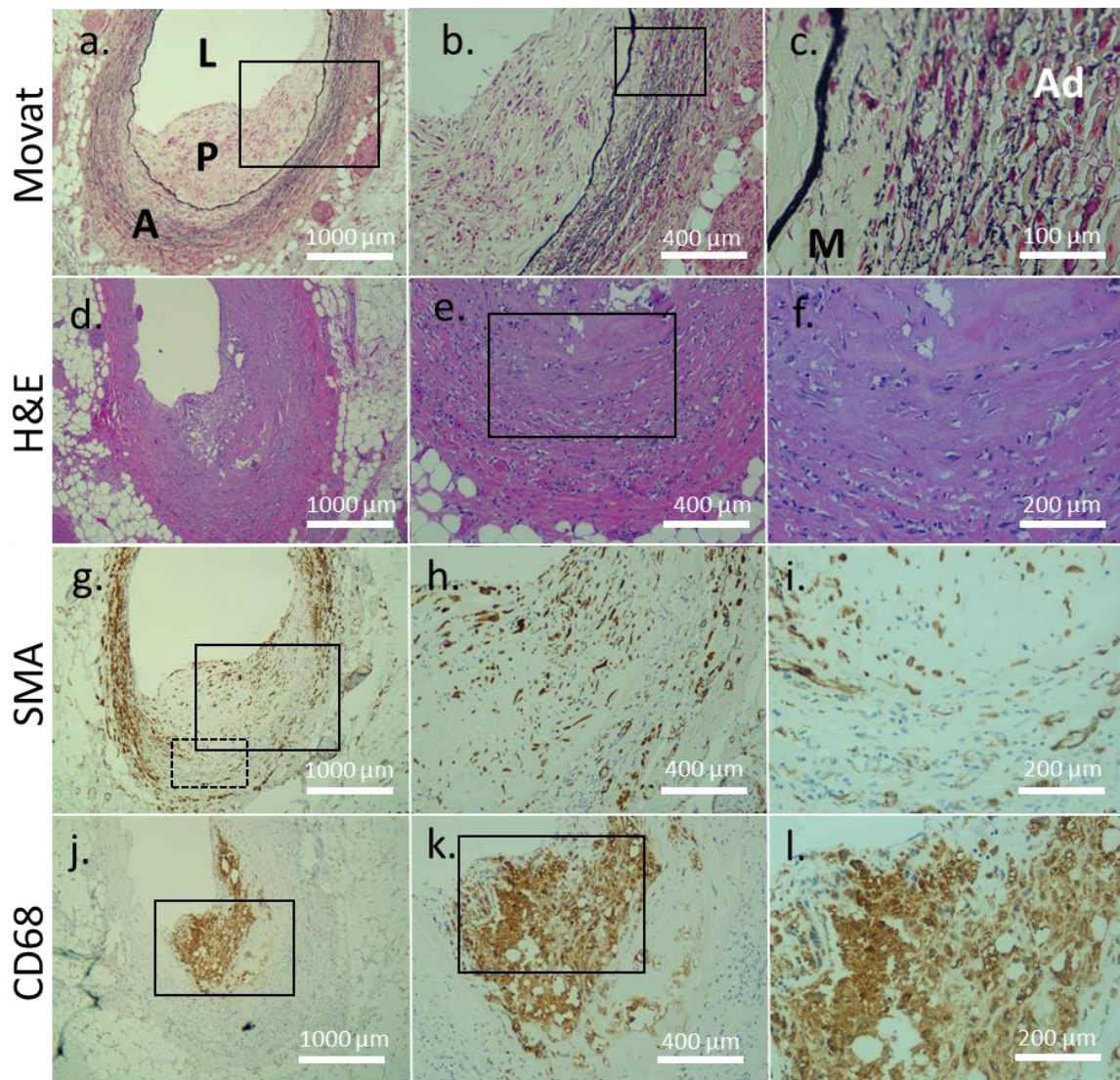


Figure 3.4. Left main coronary artery bifurcation of MOPDII patient 2. The low magnification image of the Movat staining (a) reveals a large atherosclerotic plaque (P) with residual lumen (L). Higher magnification images of the artery wall (A) reveal an absence of cells in the medial layer (M) and elastosis (b, c). H&E staining (d-f) shows similar changes. While SMA staining shows SMA-positive cells in a portion of the artery wall (g) and in the fibrous cap (h, solid box) with a paucity of SMA-positive cells in other areas of the artery wall (i, dashed box).

Histology examination was similar in that the proximal right coronary artery contained an occlusive atheromatous plaque with extensive calcification, cholesterol

crystals and SMCs, loss of medial SMCs in the region of the plaque and positive staining cells in the adventitial layer (figure 3.4).

Smooth muscle cell specific pericentrin knock-out mouse

A pericentrin smooth muscle cell specific knock-out mouse line in which a mouse carrying flox sites flanking exon 17 and 18 of *Pcnt* was obtained and crossed into a SMA-Cre-ERT2 mouse line. The resulting offspring were *Pcnt^{fl/fl}*, SMA-Cre-ERT2 (*Pcnt^{SMKO}*), where treatment with tamoxifen *in vivo* or 4-hydroxy-tamoxifen *in vitro* in turn resulted in an out-of-coding frame shift, generating a premature stop codon and a loss-of-function allele (figure 3.5a). We confirmed deletion of pericentrin in isolated SMCs with a 50% reduction in pericentrin on immunoblot analyses (figure 3.5b, c).

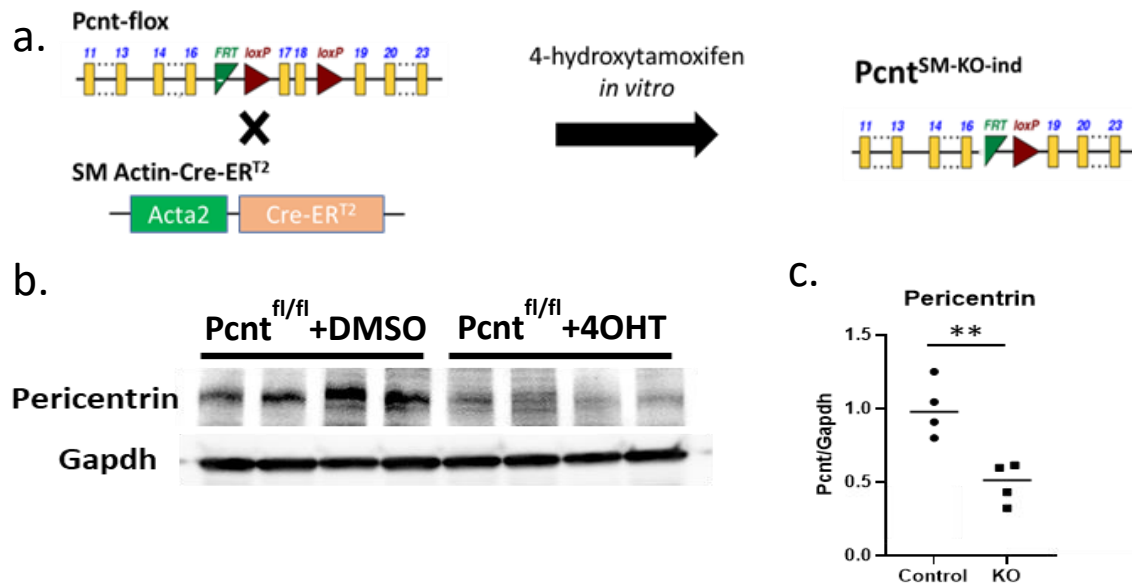
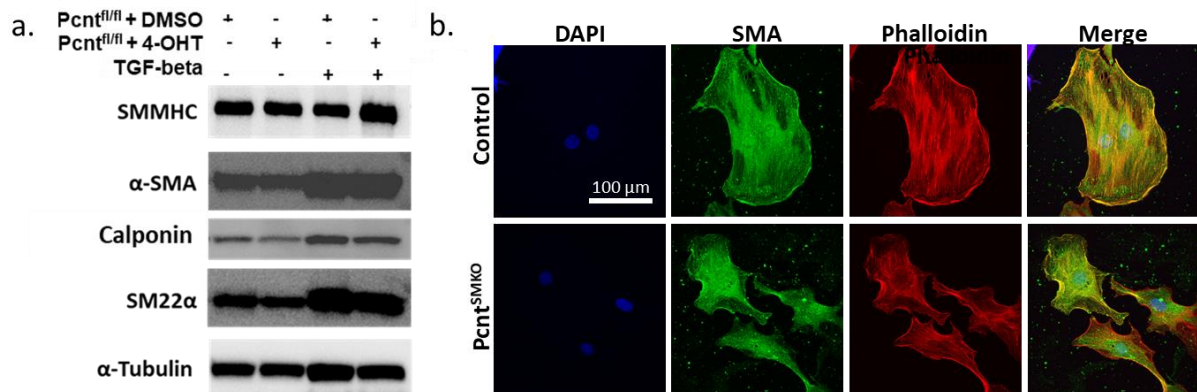


Figure 3.5. Construct of Pcnt-flox mouse and confirmation of reduction in pericentrin expression. Pcnt^{fl/fl} mice containing loxP sites flanking exon 17 and 18 of Pcnt were crossed into smooth muscle (SM) actin-Cre-ERT² mice leading to a premature stop codon and loss of function allele when treated with 4-hydroxytamoxifen (4-OHT, a). A reduction in pericentrin expression was confirmed with Western blot (b) and quantified (c).

The Pcnt^{SMKO} SMCs were harvested with and without exposure to TGF β and SMC differentiation markers assessed and the mutant SMCs had similar levels of SM α -actin, SM myosin heavy chain (SMMHC), calponin and SM22 α (figure 3.6a). Immunofluorescent staining of α -actin filaments revealed that Pcnt^{SMKO} SMCs formed organized and intact actin filaments similar to the control SMCs (figure 3.6b).



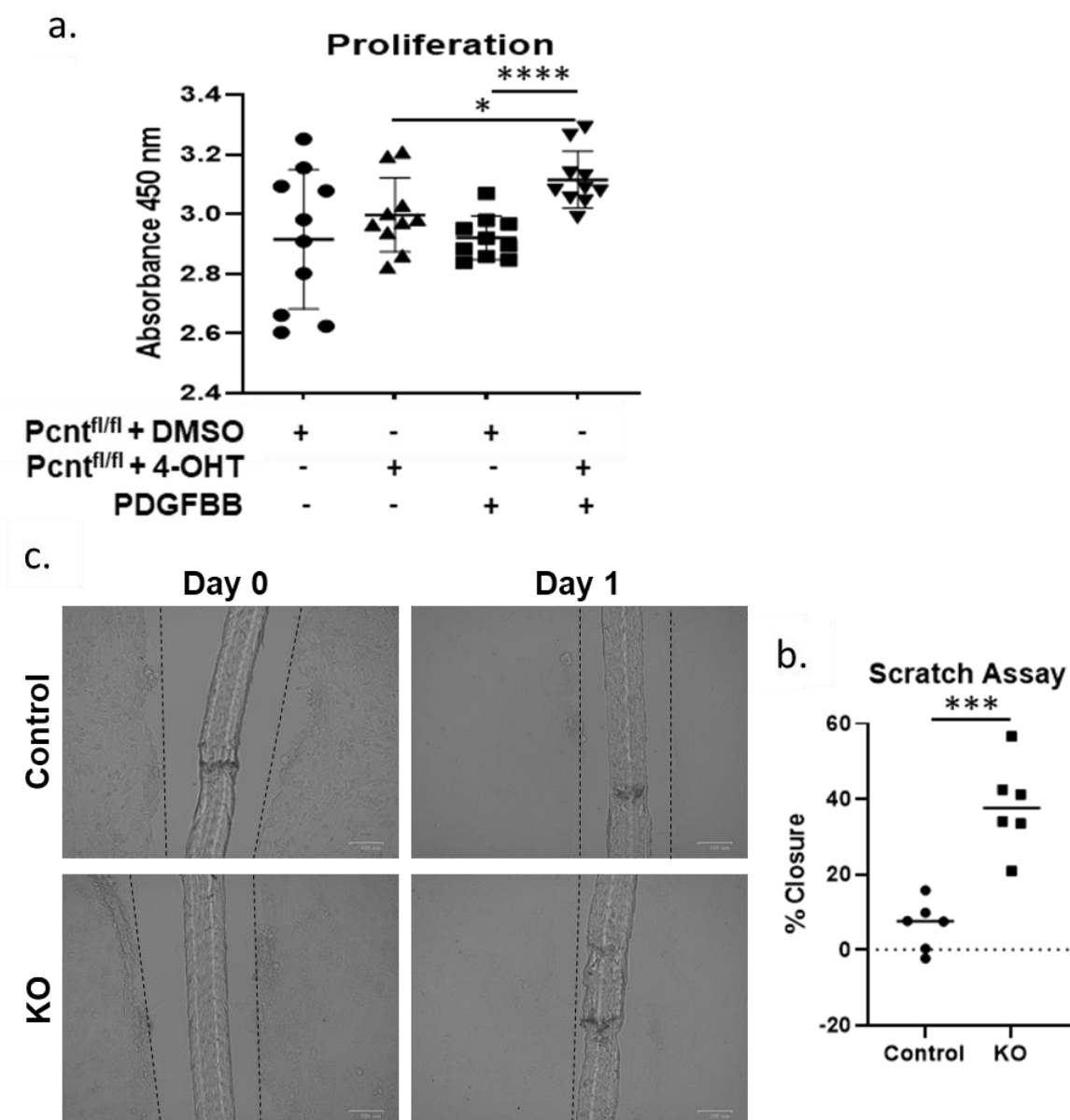


Figure 3.7. Pcnt^{SMKO} (Pcnt^{fl/fl}+4OHT) cells display increased proliferation and migration compared to DMSO treated control cells. BrdU incorporation assay shows increased proliferation of Pcnt^{SMKO} cells when treated with the SMC mitogen TGF- β (a). Wound healing scratch assay reveals increased migration of Pcnt^{SMKO} (KO) cells compared to control as seen by % closure (a, b).

Activation of ATR-Chk1 in Pcnt^{SMKO} cells

All the current hypothesis for the pathogenesis of the disease phenotype in patients with MOPDII are centered around a reduction in cellular proliferation (i.e. spindle cell misorientation, mitotic defects, ATR-Chk1 cell cycle inhibition) (Delaval and Doxsey, 2010; Chen et al., 2014a). Pericentrin plays a key role in ATR cell cycle regulation through the aiding of microcephalin recruitment of p-Chk1 to the centrosome, where p-Chk1 then acts to phosphorylate Cdc25B, deactivating it, and thus inhibiting G2 to M cell cycle progression through the accumulation of phosphorylated Cdk1/Cyclin B.

The ATR-Chk1 pathway is activated in response to oxidized cholesterol, 7-ketocholesterol, therefore we assessed whether the ATR-Chk1 pathway was activated in *Pcnt*^{SMKO} cells at baseline and in response to the cholesterol complexed to methyl- β -cyclodextrin (MBD-Chol) (Chang et al., 2016). To do so we assessed several proteins in this pathway in *Pcnt*^{SMKO} and control cells at baseline and with exposure to 2.5 or 10 μ g/ml of MBD-Chol. Total Chk1 was increased at baseline in *Pcnt*^{SMKO} cells compared to controls and was further increased with 2.5 μ g/ml MBD-Chol with corresponding elevation in p-Chk1 at baseline and with low levels of MBD-Chol (figure 3.8). This suggests that the ATR-Chk1 pathway is activated in *Pcnt*^{SMKO} cells at baseline and with low levels of cholesterol treatment. In turn, both total Cdc25B and p-Cdc35B was reduced in *Pcnt*^{SMKO} cells at baseline and with low levels of cholesterol suggesting downregulation of phosphorylation of Cdc25B by Chk1 in *Pcnt*^{SMKO} cells. Finally, both total Cdk1 and p-Cdk1 are elevated in *Pcnt*^{SMKO} cells compared to controls at baseline and with low levels of cholesterol suggesting that Cdk1 may be driving G2/M cell cycle progression in the absence of pericentrin.

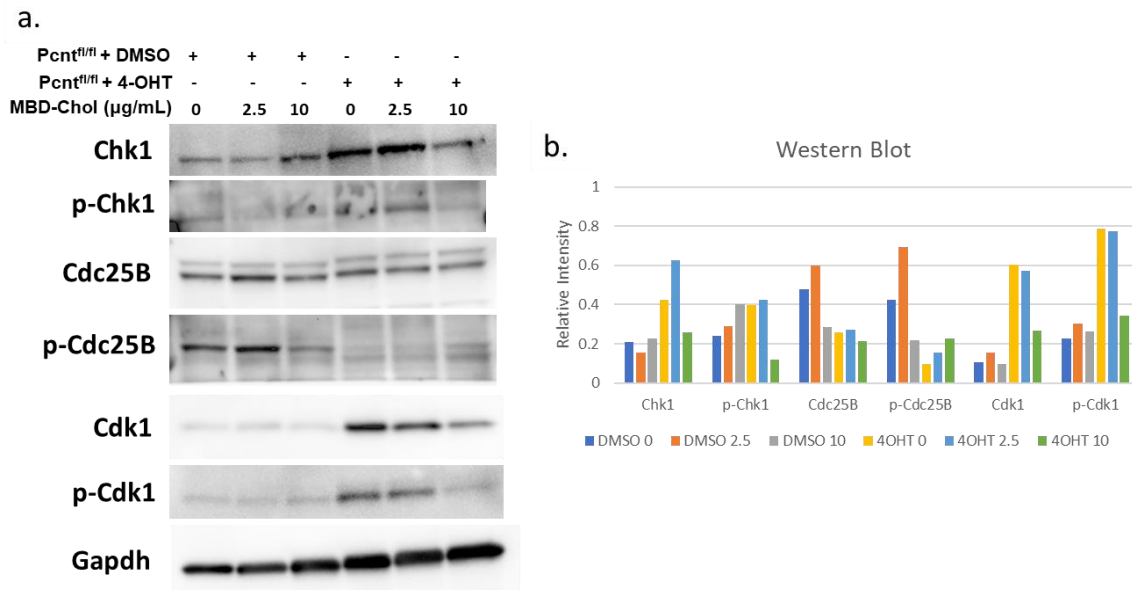


Figure 3.8. Activation of the ATR-Chk1 pathway in Pcnt^{SMKO} SMCs. Western blot analysis of 4OHT treated Pcnt^{SMKO} cells (a) shows increased activation of the ATR pathway at baseline and with cholesterol treatment with a reduction in p-Cdc25B compared to control cells and an increase in both total and p-Cdk1 (c). Protein expression of various ATR-Chk1 pathway proteins show increased expression at baseline and with cholesterol treatment in Pcnt^{SMKO} SMCs compared to controls. The reduction in p-Cdc25B in Pcnt^{SMKO} SMCs suggests that p-Chk1 is not localizing to the centrosome as hypothesized.

Pcnt^{SMKO} cells undergo phenotypic modulation when exposed to cholesterol

Our previous studies found that exposing SMCs to free cholesterol complexed to β -cyclodextrin cholesterol (MBD-chol) activates ER stress and a global unfolded protein response (UPR), which modulates the SMC phenotype that resembled modulated SMCs that appear with progression of atherosclerosis. The atherosclerosis-associated modulated SMC phenotype is characterized by decreased expression of SMC differentiation markers, and increase expression of fibroblast, macrophage and stem cell markers. We sought to determine if the Pcnt^{SMKO} SMCs upregulated atherosclerosis-associated markers of a modulated

SMC similar to control cells. *Pcnt*^{SMKO} SMCs and WT SMCs were exposed to varying levels of MD-chol. Interestingly, we found that the contractile markers *Acta2*, *Tagln*, and *Cnn1* were downregulated in *Pcnt*^{SMKO} SMCs with exposure to 2.5 ug/ml of MBD-Chol treatment whereas the WT SMCs did not downregulate these SMC markers until exposed to 10 ug/ml MD-chol (figure 3.9a). Furthermore, *Pcnt*^{SMKO} SMCs also upregulated macrophage markers *Cd68* and *Lgals3* with low levels of cholesterol treatment whereas the WT SMCs did not (figure 3.9b). Immunoblot analyses confirmed these findings (figure 3.9c).

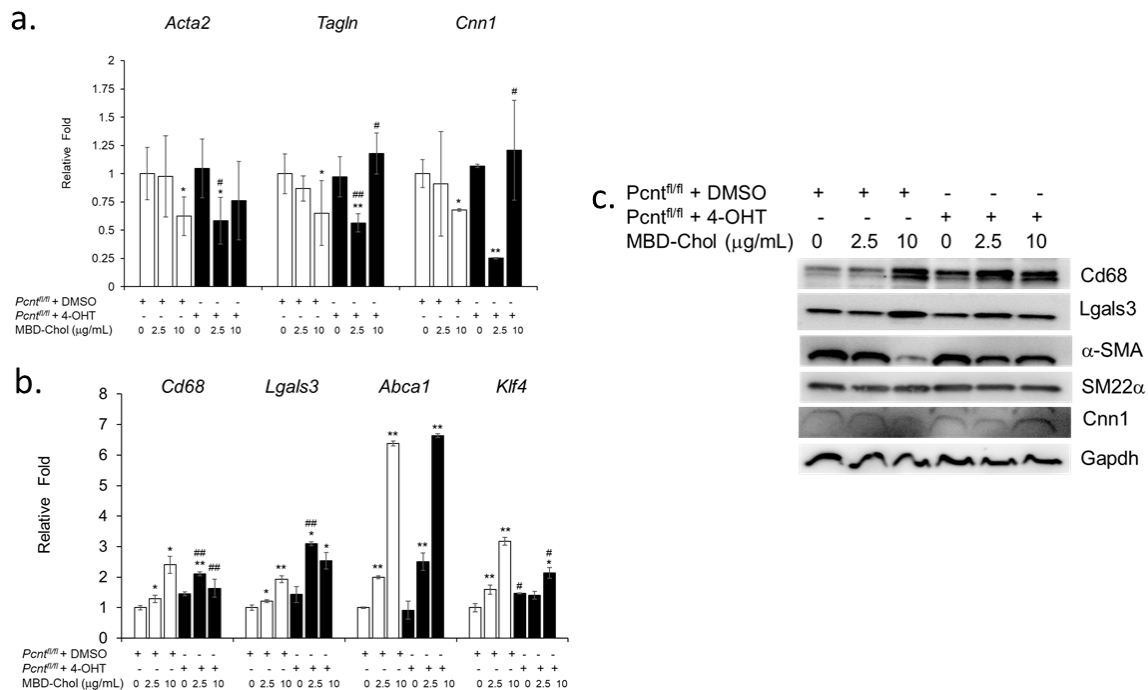


Figure 3.9. 4OHT treated *Pcnt*^{SMKO} cells display phenotypic switching. SMC contractile markers, *Acta2*, *Tagln*, and *Cnn1*, are downregulated in *Pcnt*^{SMKO} cells with low levels of cholesterol treatment compared to controls (a). While macrophage markers, *Cd68* and *Lgals3*, are increased in *Pcnt*^{SMKO} cells compared to DMSO treated control cells (b). These findings were confirmed by Western blot showing increased *Cd68* and *Lgals3* expression with decreased α -SMA and *Cnn1*. * or ** : $p < 0.05$ or $p < 0.01$, vs no cholesterol. # or ## : $p < 0.05$ or $p < 0.01$, DMSO vs 4-OHT.

In addition to modulated SMCs adopting a macrophage-like phenotype, have also been found to adopt a fibroblast- and mesenchymal stem cell-like phenotype. To assess phenotypic modulation to a fibroblast-like cell phenotype we looked at several fibroblast cell markers and found that many of them were upregulated at baseline in $Pcnt^{SMKO}$, in the absence of cholesterol treatment (figure 3.10), including *Fbn1*, *Ecrq4*, *Fmod*, *Prg4*, *Spp1*, *Timp1*, *Bgn*, *Dcn*, and *Serping1*. In addition, the mesenchymal stem cell marker *Sca1* was also upregulated at baseline and with cholesterol treatment.

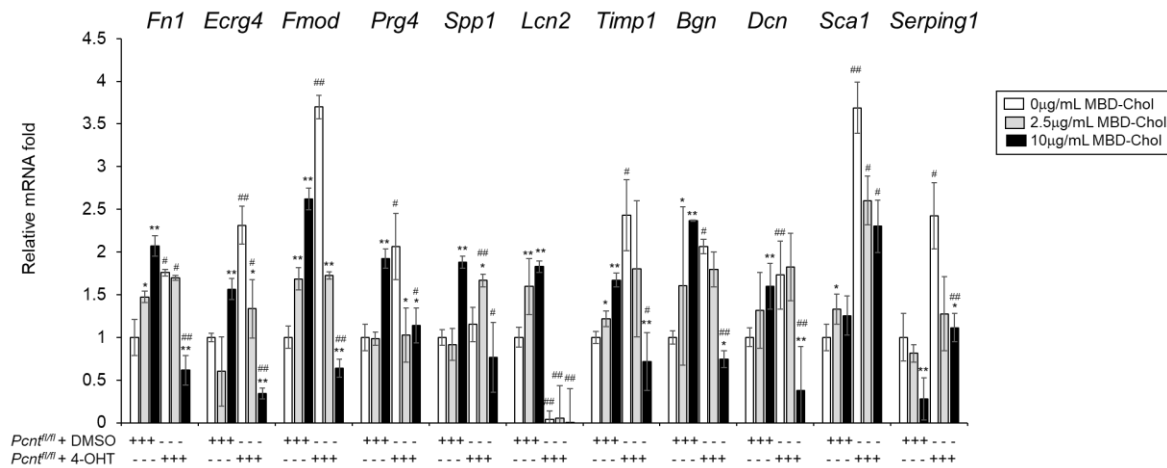


Figure 3.10. $Pcnt^{SMKO}$ cells undergo phenotypic modulation to a fibroblast- and mesenchymal-like state. Several fibroblast markers are upregulated in 4OHT-treated $Pcnt^{SMKO}$ cells at baseline (*Fn1*, *Ecrq4*, *Fmod*, *Prg4*, *Timp1*, *Bgn*, *Dcn*, and *Serping1*) and in response to cholesterol treatment (*Fn1*, *Ecrq4*, and *Spp1*). In addition, the mesenchymal stem cell marker *Sca1* is also increased at baseline and in response to cholesterol treatment. * or ** : $p < 0.05$ or $p < 0.01$, vs no cholesterol. # or ## : $p < 0.05$ or $p < 0.01$, DMSO vs 4-OHT.

Phenotypic modulation has been shown to be mediated through the UPR (Chattopadhyay et al., 2020). To investigate this potential mechanism for phenotypic modulation in $Pcnt^{SMKO}$ cells we assess markers for the three branches of the UPR: Perk, Atf6, and Ire1 α (figure 3.11). Activation of the Perk pathway was indicated by

elevation of *Atf4* in presence of low levels of cholesterol, although *Chop*, another downstream product of the Perk pathway, was not significantly elevated compared to control. In addition to activation of the Perk pathway, there was also evidence of activation of the Atf6 arm of the UPR as evidenced by elevations in both *Grp94* and *Bip* in *Pcnt*^{SMKO} cells in the presence of low levels of cholesterol. Finally, the Ire1a pathway was also activated as seen by increased levels of *Edem* in *Pcnt*^{SMKO} cells in the presence of low levels of cholesterol in conjunction with increased *sXbp1*.

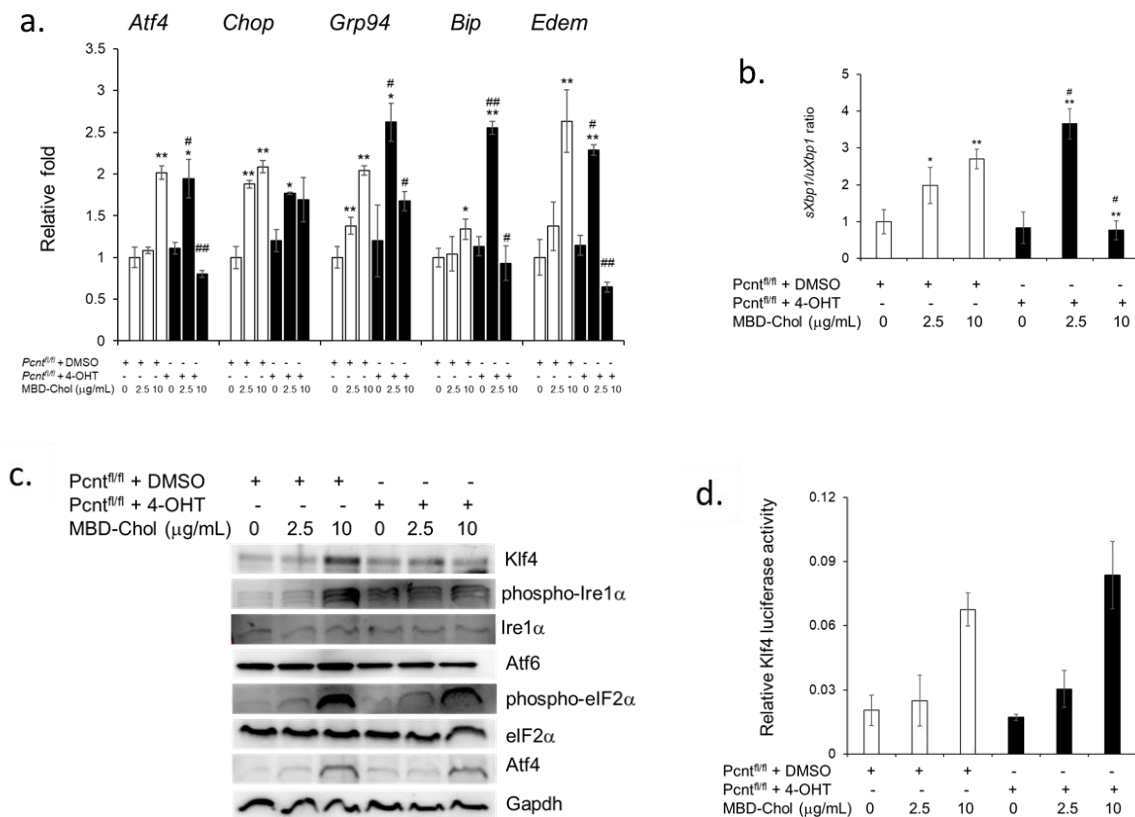


Figure 3.11. *Pcnt*^{SMKO} cells show activation of Unfolded Protein Response (UPR) pathways. *Atf4*, *Grp94*, *Bip*, and *Edem* are all upregulated in response to low levels of cholesterol (a) suggesting activation of all three UPR pathways. *sXbp1* is also elevated with cholesterol (b) suggesting activation of Ire1α. In addition, p-Ire1α is elevated on Western blot (c). While there is no difference in Klf4 activation between 4OHT-treated *Pcnt*^{SMKO} cells and DMSO-treated control cells (d). * or **: $p < 0.05$ or $p < 0.01$, vs no cholesterol. # or ## : $p < 0.05$ or $p < 0.01$, DMSO vs 4-OHT.

Unpublished data from our laboratory has shown activation of cytosolic stress pathways in modulated SMCs. With this in mind, we assessed cytosolic stress in the *Pcnt*^{SMKO} cells to identify if this may also be driving phenotypic modulation in these cells. Interestingly, the heat shock transcription factor *Hsf1*, and all three heat shock gene transcripts examined, *Hsp70*, *Hsp90aa1*, and *Hsp90ab1*, were significantly upregulated at baseline (figure 3.12a). This was confirmed by Western blot analysis of Hsp90 and Hsp70 which were also upregulated at baseline, prior to cholesterol treatment in *Pcnt*^{SMKO} cells (figure 3.12c). Finally, we assessed activation of the heat shock element by Hsf1 using a dual luciferase activity assay and found that HSE activation was up at baseline and with low levels of cholesterol treatment in *Pcnt*^{SMKO} mice compared to controls (figure 3.12b). These findings suggest that *Pcnt*^{SMKO} cells undergo phenotypic modulation at a higher rate than controls at low levels of cholesterol and that this modulation is due to activation of the UPR and/or cytosolic stress.

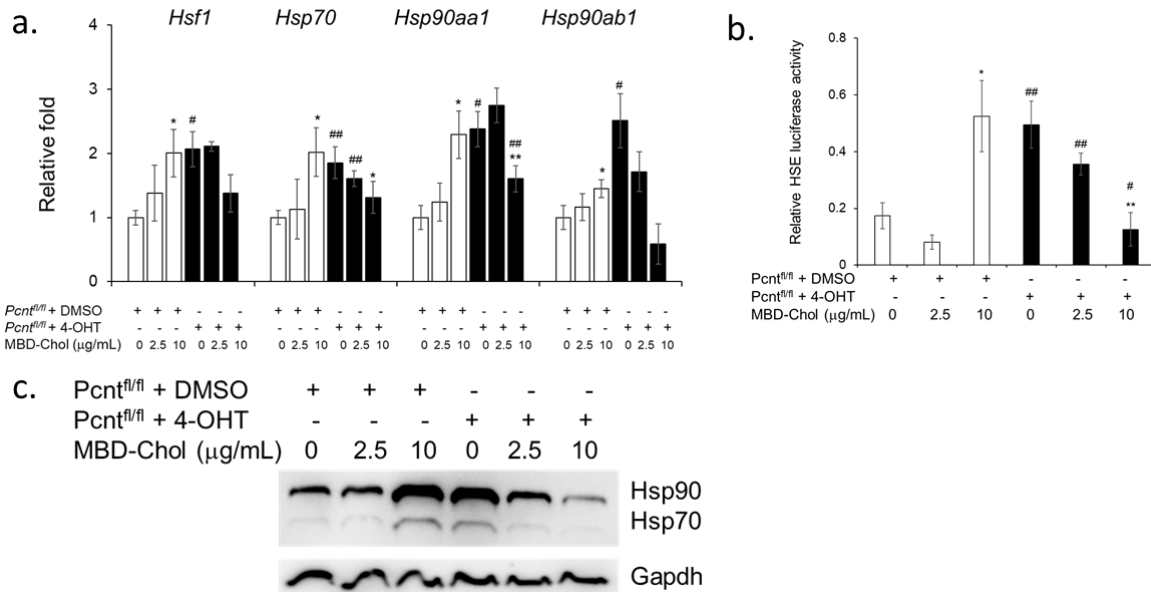


Figure 3.12. Cytosolic stress pathways are significantly elevated at baseline in 4OHT-treated $Pcmt^{SMKO}$ SMCs compared to DMSO-treated control cells. The heat shock transcription factor, *Hsf1*, along with the heat shock proteins *Hsp70*, *Hsp90aa1*, and *Hsp90ab1* are all elevated at baseline in $Pcmt^{SMKO}$ cells (a). *Hsf1* activation of heat shock element (HSE) is also increased at baseline and with cholesterol treatment in $Pcmt^{SMKO}$ cells (b). Finally, these findings were confirmed by Western blot with both *Hsp70* and *Hsp90* having increased protein expression at baseline in $Pcmt^{SMKO}$ cells (c).

Pcmt^{SMKO} mice do not have aortic dilatation or alterations in cardiac output

Echocardiography was performed and aortic and cardiac parameters evaluated. No aortic enlargement was observed in $Pcmt^{SMKO}$ mice compared to controls, either at the aortic root or the ascending aorta (figure 3.13 a-c). Cardiac output was also unchanged in $Pcmt^{SMKO}$ mice compared to controls (figure 1.13d). Consistent with this finding there was also no significant difference in systolic or diastolic cardiac diameter and left ventricular volume, or ejection fraction.

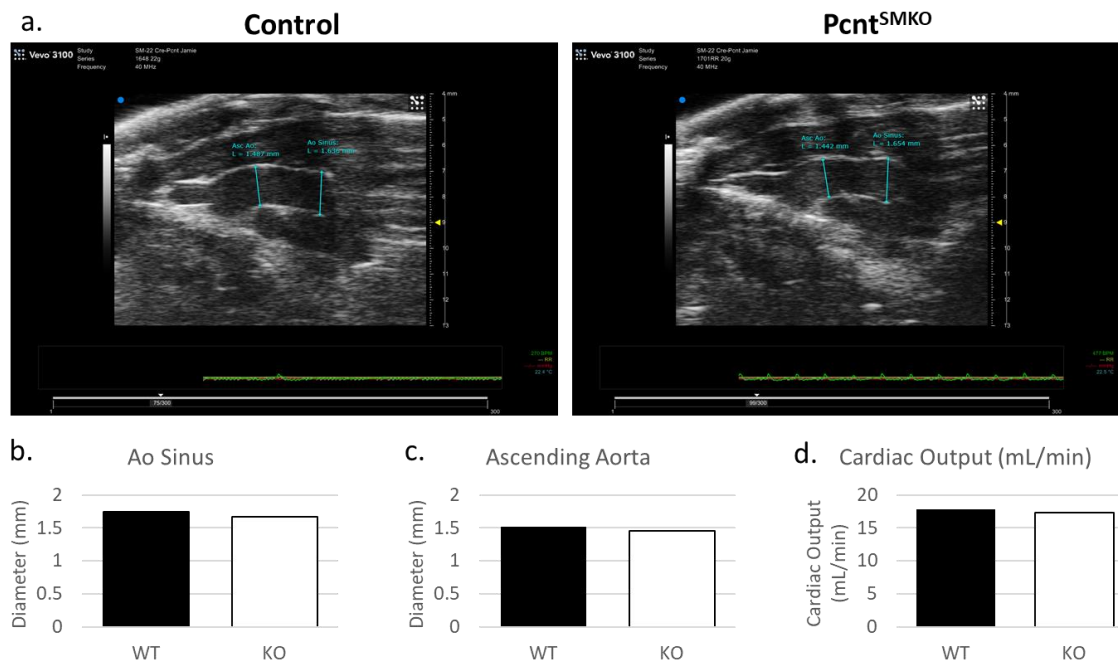


Figure 3.13. $Pcnt^{SMKO}$ mice do not have aortic dilatation or cardiac dysfunction on echocardiography. There was no significant differences in aortic sinus or ascending aortic diameter (a-c) or cardiac output (d) on echocardiography.

$Pcnt^{SMKO}$ mice develop atherosclerotic disease in vivo

To study the development of atherosclerotic disease *in vivo* we utilized a constitutive SM22 α -Cre in conjunction with our $Pcnt$ -flox mice to enable knock-out of $Pcnt$ from the beginning of development. Studies have shown that a single injection of adeno-associated virus (AAV) expressing a gain-of-function mutation in PCSK9 ($PCSK9^{DY}$) leads to sustained hypercholesterolemia when the mice are fed a high fat diet, and the subsequent atherosclerotic plaque burden is similar to that observed in the $Ldlr^{-/-}$ mice with a similar diet (Roche-Molina et al., 2015). We injected 6-week-old mice with AAV- $PCSK9^{DY}$ and then fed a high fat diet for 14 weeks. En face whole aorta Oil Red O staining showed significantly more atherosclerotic disease in the $Pcnt^{fl/fl}$, SM22 α -Cre mice compared to $Pcnt^{fl/fl}$ control mice (figure 3.14). It should be noted that two outlying values, one per group, were excluded due to possible overstaining. With these values included the difference in staining between the groups was not statistically significant. There was no statistically significant difference in weight or cholesterol level.

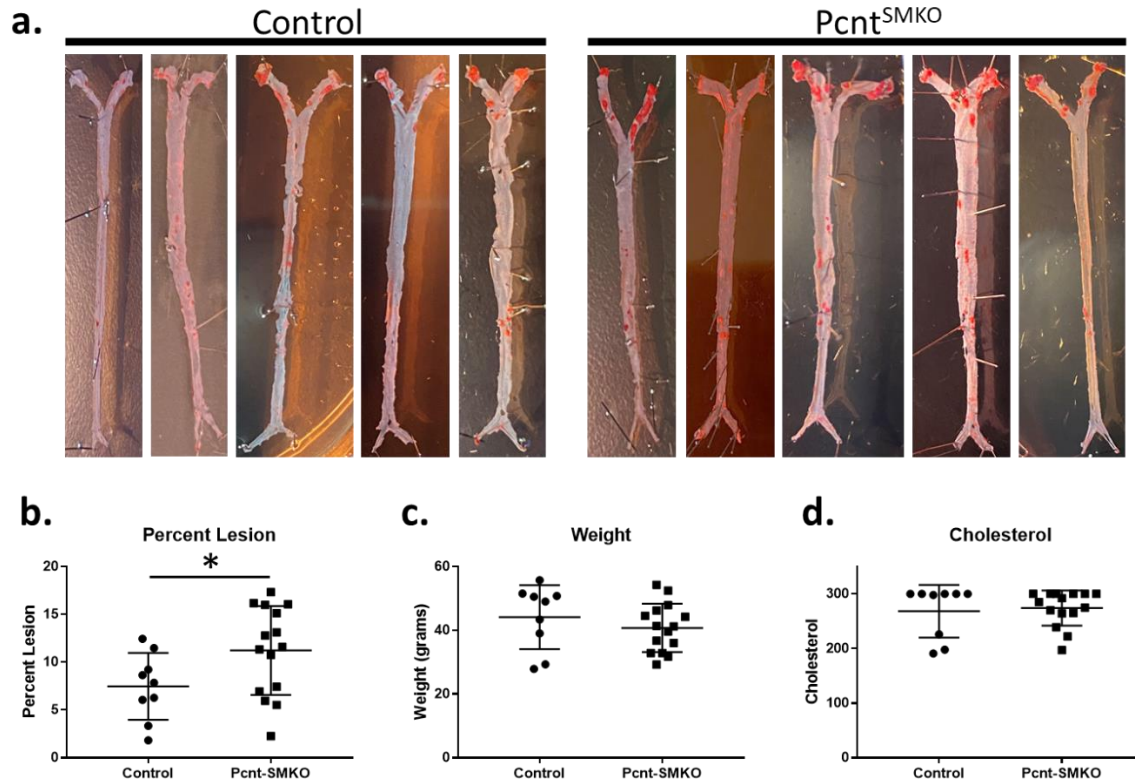


Figure 3.14. Atherosclerotic disease in Pcnt^{SMKO} mice following AAV-PCSK9^{DY} and high fat diet. Representative Oil Red O stained whole aortas from mice administered a single injection of AAV-PCSK9^{DY} and fed high fat diet for 14 weeks (a). Oil Red O staining was quantified in ImageJ and the percent lesion was calculated (b). Pcnt^{SMKO} mice had significantly more atherosclerotic disease burden compared to control mice (p=0.0479). Weights were measured prior to aorta collection. There was no significant difference in weight between Pcnt^{SMKO} and control mice (c). Non-fasting cholesterol level was measured prior to sacrifice (maximum measurement 300). There was no significant difference in cholesterol level between Pcnt^{SMKO} and control mice (d).

Discussion

Here we describe coronary artery pathology from two patients with MOPDII. These patients have a particularly severe atherosclerotic phenotype given their young age. While patient 1 did have a history of hypercholesterolemia and hypertension, the degree of coronary artery disease seen is out of proportion to his relatively young age and absence of other risk factors such as smoking,

hypertension, diabetes mellitus, and obesity (Herrington et al., 2016). In addition to the severe atherosclerotic disease in these patients were changes not commonly seen with atherosclerosis, particularly the loss of SMCs within the medial layer. Human coronary arteries normally have multiple layers of SMCs, but the coronary arteries of both patients presented here showed a marked reduction in SMCs in the medial layer, with greater than expected numbers of SMA-positive cells in the adventitial layer and a population of SMA-positive cells in the fibrous cap of the atherosclerotic plaques (Sharma et al., 2017).

There are a few possibilities for the marked reduction in SMCs in the medial layer, the first being abnormalities in artery development. SMCs are recruited to the endothelial layer during artery wall development through PDGFB signaling (Udan et al., 2013). Alterations in the recruitment would explain the paucity of SMCs in the medial layer but not the presence of SMA-positive cells within the adventitia and fibrous cap. Another possibility is that SMCs originally migrate to the medial layer and then due to factors yet to be determined, migrate out from the medial layer to the adventitial layer and fibrous cap of the atheroma, explaining the large numbers of SMA-positive cells in these locations. Finally, another possibility is that while some SMCs migrate into the atheroma and fibrous cap, some SMCs remain behind and become apoptotic. The SMCs present in the medial layer were noted to appear vacuolated and “sick”. This raises the possibility that those SMCs remaining in the medial layer are abnormal and undergo apoptosis at a high rate, while SMCs that migrate out of the medial layer and undergo phenotypic modulation have a survival advantage.

Also of note in MOPDII patient coronary arteries is the degree of elastosis in the adventitial layer. The proximal coronary arteries are muscular and therefore typically contain to elastin layers, the internal and external elastic laminae, with the external elastic lamina being absent in the smallest of the muscular arteries (Cocciolone et al., 2018). The elastin precursor, tropoelastin, is primarily produced by SMCs within the media, but may also be produced by endothelial cells in the intima and fibroblasts in the adventitia (Cocciolone et al., 2018). The elastin deposition within the adventitial layer may be produced by either SMCs or myofibroblasts.

The increased proliferation observed by $Pcnt^{SMKO}$ SMCs was surprising given that all of the currently posited hypothesis for the clinical manifestations of MOPDII are centered around decreased cellular proliferation (Griffith et al., 2008; Delaval and Doxsey, 2010; Chen et al., 2014b). Here we investigate a potential role for the ATR-Chk1 pathway in increased SMC proliferation. Of note, total Cdk1 was found to be increased in $Pcnt^{SMKO}$ SMCs in addition to p-Cdk1. Increased Cdk1 is observed in multiple cancers suggesting a role in abnormal cellular proliferation (Hansel et al., 2005; Kang et al., 2014; Yang et al., 2014; Zhang et al., 2018).

All three ER stress pathways, Perk, Atf6, and Ire1a, are activated with low levels of cholesterol treatment in $Pcnt^{SMKO}$ SMCs. In addition, the heat shock response pathway is upregulated at baseline and with low levels of cholesterol treatment. Cholesterol-induced phenotypic switching has been shown to be associated with UPR activation with inhibition of the UPR preventing phenotypic switching in SMCs (Chattopadhyay et al., 2020). Hsp70 is known to interact with

Pcnt at the centrosome (Fang et al., 2019). One potential hypothesis for activation of the heat shock response at baseline in Pcnt^{SMKO} SMCs is that absence of the scaffold function of pericentrin at the centrosome leads to activation of the heat shock response. This would explain the increased activation of the heat shock response at baseline. Hsp70 in turn negatively regulated Hsf1, a potential mechanism for the decrease in heat shock response with cholesterol treatment.

The heat shock response is also linked to the ATR-Chk1 pathway. Treatment with the heat shock protein inhibitor phenethyl isothiocyanate (PEITC) reduced levels of CDK1 leading to G2/M cell cycle arrest and apoptosis in a human breast cancer cell line in addition to reducing levels of HSF1, HSP70 and HSP90 (Sarkars et al., 2013). This suggests a link between the heat shock response and CDK1-mediated G2/M checkpoint regulation. This makes PEITC a potentially promising pharmacologic treatment for the inhibition of both the ATR-Chk1 pathway and the heat shock response in MOPDII.

Chapter Four: Discussion

The study of rare genetic disorders such as SMDS and MOPDII are crucial not only to our understanding of their pathophysiology and to the development of better treatments for these conditions, but also to our understanding of more common conditions. Vascular diseases are complex, but by studying rare conditions in which vascular pathology is prevalent and severe we may then better understand the more common types of vascular pathology leading to coronary artery disease, aortic aneurysm, cerebral infarcts, and Moyamoya disease just to name a few of these diverse vascular pathologies.

Vascular smooth muscle cells are particularly unique in their ability to de-differentiate and, as we discuss here, modulate their phenotype in response to stimuli. Better understanding this process, what causes it, and how it contributes to the development of disease helps us to understand the pathophysiology of vascular disease. This in turn furthers the development of novel therapeutics for these conditions.

Smooth Muscle Dysfunction Syndrome

Here we described hepatic and pulmonary pathology in three patients with SMDS, including expansion of the portal triads, thickening of the terminal branches of the hepatic artery, arterial changes consistent with pulmonary hypertension, and emphysematous changes suggestive of abnormal pulmonary development. To further study the pathogenesis of vascular disease associated with mutations in *ACTA2* R179 our laboratory developed a novel mouse model. Using this mouse model, we can evaluate the lung histology and multiple time points from embryonic development into adulthood to determine if the pulmonary changes observed in the

three patients with SMDS also occur in the mouse model and whether these changes are developmental in origin. We can also further characterize the liver changes observed in patients with SMDS by studying the liver histology using this mouse model along with the expression of specific cells, particularly SMA-expressing stellate cells. These findings suggest a crucial role for SMCs in lung alveolar development and may shed light on other diseases of the lung parenchyma, including other causes of emphysema and cystic lung disease.

In addition, using SMCs isolated from *Acta2* R179 mutant mice, we can study their phenotype *in vitro*, including contractile protein expression, proliferation, and migration. Furthermore, we can assess whether these mutant cells undergo phenotypic modulation when exposed to cholesterol similar to *Pcnt*^{SMKO} and other cell lines our laboratory is studying. Based on the pathology observed in the patient samples from patients with SMDS described here we would expect to see increased proliferation and migration of the mutant cells *in vitro*. These patients do not have a higher rate of atherosclerotic disease, as seen in other models which undergo phenotypic modulation, so we would not expect phenotypic modulation with cholesterol treatment in these cells.

Majewski Osteodysplastic Primordial Dwarfism Type II

The studies of the coronary artery tissue from patients with MOPDII brought up several interesting questions that our laboratory can continue to pursue. One question is whether the findings we observed in the coronary artery tissue, including dropout of SMCs in the medial layer, increased SMA positive cells in the adventitia, and elastosis in the adventitia are specific to the coronary vascular bed. If similar

pathology is present in other arteries, that would suggest a unifying mechanism for the diverse vascular pathologies observed in patients with MOPDII, including aortic and cerebral aneurysms, and moyamoya disease.

In addition, the cause of dropout of SMCs in the medial layer of the coronary arteries is yet to be elucidated. Histology of vessel tissue from Pcnt^{SMKO} mice may shed light on this by determining if this finding is recapitulated in the context of smooth muscle cell-specific knock-out of pericentrin. If so, we can then assess the presence and location of SMCs in the vessel wall during development and perform apoptosis assays to determine if this finding is a result of decreased SMC development, increased SMC cell death, or dysregulated cell migration. In addition, it would be insightful to determine whether arteries from Pcnt^{SMKO} mice show increased elastin deposition like that observed in the MOPDII patient coronary artery tissue.

Another question that still needs to be more fully explored is the exact role of the ATR-Chk1 pathway in patients with MOPDII. Our findings show an increase in ATR activation with a corresponding increase in Cdk1 and p-Cdk1 levels. Cdk1 levels typically do not vary widely, but overexpression has been observed in some cancers, including melanomas and diffuse large B-cell lymphomas (Roskoski, 2019). Further, data from other labs have shown a relationship between the heat shock response pathway and Cdk1 cell cycle regulation (Sarkars et al., 2013). Finally, Cdk1 has been shown to enhance protein synthesis at least in part through eIF2 α (Haneke et al., 2019). These findings suggest that Cdk1 may be a potential target for inhibition of the increased proliferation observed in Pcnt^{SMKO} SMCs. Several agents

with inhibitory effects on Cdk1 have been developed for cancer therapeutics, although none are specific to Cdk1 alone (Lin et al., 2009; Parry et al., 2010; Paruch et al., 2010; Zeidner et al., 2015; Roskoski, 2016). These agents should be tested to determine if inhibition of Cdk1 activity reduces proliferation in Pcnt^{SMKO} SMCs.

All three pathways of the UPR were activated in Pcnt^{SMKO} SMCs with low levels of cholesterol. Previous studies in our laboratory in wild-type SMCs have shown that phenotypic modulation is dependent on activation of the UPR (Chattopadhyay et al., 2020). To further investigate the role of each UPR pathway in phenotypic modulation of Pcnt^{SMKO} SMCs the next step would be to treat them *in vitro* with agents targeting the UPR. To delineate the specific UPR pathways involved in phenotypic modulation of Pcnt^{SMKO} SMCs, we would treat with the integrative stress response inhibitor ISRIB, which blocks phosphorylation of eIF2a and the downstream activation of ATF4, Ceapin A7 to inhibit the cleavage and activation of ATF6, and finally Kira6 for the inhibition of Ire1 α (Palam et al., 2015; Mahameed et al., 2019; Xue et al., 2021). Based on the current data, we expect that all three UPR pathways are involved in phenotypic modulation of Pcnt^{SMKO} SMCs with inhibiting one or all of these pathways leading to alteration of phenotypic modulation.

Finally, next steps would also be to investigate the role of cytosolic stress in phenotypic modulation in Pcnt^{SMKO} SMCs. As shown in chapter 3, Hsf1, Hsp70, and Hsp90 are all upregulated at baseline in Pcnt^{SMKO} SMCs suggesting cytosolic stress in these cells at baseline and with low levels of cholesterol. Additionally, Hsp70 is known to interact with pericentrin at the centrosome, suggesting that loss of function

mutations in *Pcnt* drive cytosolic stress through Hsp70. To investigate this further, we should go on to treat *Pcnt*^{SMKO} SMCs with cytosolic stress inhibitors and determine the effect on SMC phenotypic modulation, proliferation, and migration. These inhibitors should include 17-allyloamino-17-demethoxygeldanamycin (17-AAG), a selective inhibitor of Hsp90 and Phenethyl isothiocyanate (PEITC), which downregulates expression of Hsf1 in addition to inhibiting Cdk1 which, as discussed previously, is also upregulated at baseline in *Pcnt*^{SMKO} SMCs (Sarkars et al., 2013).

Conclusion

Here we have discuss novel insights into Smooth Muscle Dysfunction Syndrome and Majewski Osteodysplastic Primordial Dwarfism Type II. Mutations in *ACTA2* lead to diverse, widespread vascular disease, including occlusive vascular pathology (Guo et al., 2009; Papke et al., 2013). In addition to the known vascular pathology caused by mutations in *ACTA2* R179, we also found pulmonary developmental abnormalities likely due to loss of *ACTA2* expression in SMCs during pulmonary segmental branching morphogenesis (Danopoulos et al., 2018; Goodwin et al., 2019). In addition, these patients display thickening of the terminal branches of the hepatic artery and expansion of the portal triads. As discussed, these findings suggest multiple avenues for future research utilizing our *Acta2* R179 mouse model.

Here we also describe how SMC-specific knockout of pericentrin leads to increased SMC proliferation and migration. This may be due in part to dysregulation of the ATR-Chk1 pathway as a result of loss of pericentrin leading to increased Cdk1. We also found that loss of pericentrin leads to phenotypic modulation of SMCs when exposed to cholesterol with decreased expression of SMC markers and

increased expression of macrophage, fibroblast and mesenchymal stem cell markers. All three of these cellular behaviors underly occlusive vascular disease pathogenesis.

This work expands our understanding of rare vascular disease pathogenesis and provides novel avenues for future scientific study. This includes further study of the impact of the *Acta2* R179 mutation on pulmonary development. There is also potential for the use of Cdk1 or Hsf1 inhibitors in the management of MOPDII. These findings also suggest a potentially pivotal role for ATR-Chk1 cell cycle regulation in SMC proliferation and show further evidence of phenotypic modulation in atherosclerotic disease development.

There are still multiple avenues of future research to be explored based on these findings, including both *in vitro* and *in vivo* studies using pathway-specific inhibitors as described above. These findings could eventually contribute to novel therapies for the prevention of vascular disease development in patients with SMDS and MOPDII. In addition, these findings broaden our knowledge of the role of phenotypic modulation in vascular disease pathogenesis and potential avenues for new therapies for atherosclerotic vascular disease.

References

- Abifadel M et al. (2003) Mutations in PCSK9 cause autosomal dominant hypercholesterolemia. *Nat Genet* 34:154–156.
- Ahotupa M (2017) Oxidized lipoprotein lipids and atherosclerosis. *Free Radic Res* 51:439–447.
- Alberts B, Johnson A, Lewis J, Morgan D, Raff M, Roberts K, Walter P (2015) *Molecular Biology of the Cell, Sixth*. New York, NY: Garland Science, Taylor & Francis Group, LLC.
- Albornoz G, Coady MA, Roberts M, Davies RR, Tranquilli M, Rizzo JA, Elefteriades JA (2006) Familial Thoracic Aortic Aneurysms and Dissections-Incidence, Modes of Inheritance, and Phenotypic Patterns. *Ann Thorac Surg* 82:1400–1405.
- Alena Moiseenko, Kheirollahi V, Cho-Ming Chao A, Quantius J, Wilhelm J, Herold S, Ahlbrecht K, Morty RE, Rizvanov AA, Minoo P, Agha E El, Bellusci S (2017) Origin and Characterization of Alpha Smooth Muscle Actin-Positive Cells During Murine Lung Development. *Stem Cells* 35:1566–1578.
- Alencar GF et al. (2020) Stem Cell Pluripotency Genes Klf4 and Oct4 Regulate Complex SMC Phenotypic Changes Critical in Late-Stage Atherosclerotic Lesion Pathogenesis. *Circulation*:2045–2059.
- Arnett DK, Blumenthal RS, Albert MA, Buroker AB, Goldberger ZD, Hahn EJ, Himmelfarb CD, Khera A, Lloyd-Jones D, McEvoy JW, Michos ED, Miedema MD, Muñoz D, Smith SC, Virani SS, Williams KA, Yeboah J, Ziaeian B (2019) 2019 ACC/AHA Guideline on the Primary Prevention of Cardiovascular

Disease: A Report of the American College of Cardiology/American Heart Association Task Force on Clinical Practice Guidelines.

Barna J, Csermely P, Vellai T (2018) Roles of heat shock factor 1 beyond the heat shock response. *Cell Mol Life Sci* 75:2897–2916 Available at: <https://doi.org/10.1007/s00018-018-2836-6>.

Bennett MR, Sinha S, Owens GK (2016) Vascular Smooth Muscle Cells in Atherosclerosis. *Circ Res* 118:692–702.

Bentzon JF, Otsuka F, Virmani R, Falk E (2014) Mechanisms of plaque formation and rupture. *Circ Res* 114:1852–1866.

Bober MB, Jackson AP (2017) Microcephalic Osteodysplastic Primordial Dwarfism, Type II: a Clinical Review. *Curr Osteoporos Rep* 15:61–69.

Bober MB, Khan N, Kaplan J, Lewis K, Feinstein JA, Jr CIS, Steinberg GK (2010) Majewski Osteodysplastic Primordial Dwarfism Type II (MOPD II): Expanding the Vascular Phenotype. :960–965.

Boileau C et al. (2012) TGFB2 mutations cause familial thoracic aortic aneurysms and dissections associated with mild systemic features of Marfan syndrome. *Nat Genet* 44:916–921 Available at: <http://dx.doi.org/10.1038/ng.2348>.

Brancati F, Castori M, Mingarelli R, Dallapiccola B (2005) Majewski Osteodysplastic Primordial Dwarfism Type II (MOPD II) Complicated by Stroke: Clinical Report and Review of Cerebral Vascular Anomalies. *Am J Med Genet A* 139A:212–215.

Bravo R, Parra V, Gatica D, Rodriguez AE, Torrealba N, Paredes F, Wang Z V, Zorzano A, Hill JA, Jaimovich E, Quest AFG, Lavandero S (2013) Endoplasmic

Reticulum and the Unfolded Protein Response. Dynamics and Metabolic Integration. *Int Rev Cell Mol Biol* 301:215–290.

Brodsky MC, Turan KE, Khanna CL, Patton A, Kirmani S (2014) Congenital mydriasis and prune belly syndrome in a child with an ACTA2 mutation. *J AAPOS* 18:393–395.

Byers PH, Holbrook KA, Barsh GS, Smith LT, Bornstein P (1981) Altered secretion of type III procollagen in a form of type IV Ehlers-Danlos syndrome. :336–341.

Chang MC, Chen YJ, Liou EJW, Tseng WY, Chan CP, Lin HJ, Liao WC, Chang YC, Jeng PY, Jeng JH (2016) 7-Ketocholesterol induces ATM/ATR, Chk1/Chk2, PI3K/Akt signalings, cytotoxicity and IL-8 production in endothelial cells. *Oncotarget* 7:74473–74483.

Chattopadhyay A, Kwartler CS, Kaw K, Li Y, Kaw A, Chen J, Lemaire SA, Shen YH, Milewicz DiM (2020) Cholesterol-Induced Phenotypic Modulation of Smooth Muscle Cells to Macrophage/Fibroblast-like Cells Is Driven by an Unfolded Protein Response. *Arterioscler Thromb Vasc Biol*:302–316.

Chen CT, Hehnly H, Yu Q, Farkas D, Zheng G, Redick SD, Hung HF, Samtani R, Jurczyk A, Akbarian S, Wise C, Jackson A, Bober M, Guo Y, Lo C, Doxsey S (2014a) A Unique Set of Centrosome Proteins Requires Pericentrin for Spindle-Pole Localization and Spindle Orientation. *Curr Biol* 24:2327–2334.

Chen CT, Hehnly H, Yu Q, Farkas D, Zheng G, Redick SD, Hung HF, Samtani R, Jurczyk A, Akbarian S, Wise C, Jackson A, Bober M, Guo Y, Lo C, Doxsey S (2014b) A Unique Set of Centrosome Proteins Requires Pericentrin for Spindle-Pole Localization and Spindle Orientation. *Curr Biol* 24:2327–2334 Available at:

<http://dx.doi.org/10.1016/j.cub.2014.08.029>.

Cocciolone AJ, Hawes JZ, Staiculescu MC, Johnson EO, Murshed M, Wagenseil JE (2018) Elastin, arterial mechanics, and cardiovascular disease. *Am J Physiol - Hear Circ Physiol* 315:H189–H205.

Danopoulos S, Alonso I, Thornton ME, Grubbs BH, Bellusci S, Warburton D, Al Alam D (2018) Human lung branching morphogenesis is orchestrated by the spatiotemporal distribution of ACTA2, SOX2, and SOX9. *Am J Physiol - Lung Cell Mol Physiol* 314:L144–L149.

Delaval B, Doxsey SJ (2010) Pericentrin in cellular function and disease. 188:181–190.

Demyanenko S, Uzdensky A (2017) Profiling of Signaling Proteins in Penumbra After Focal Photothrombotic Infarct in the Rat Brain Cortex. *Mol Neurobiol* 54:6839–6856.

Dickie R, Wang YT, Butler JP, Schulz H, Tsuda A (2007) Distribution and quantity of contractile tissue in postnatal development of rat alveolar interstitium. *Anat Rec* 291:83–93.

Dubland JA, Francis GA (2016) So Much Cholesterol: The unrecognized importance of smooth muscle cells in atherosclerotic foam cell formation. *Curr Opin Lipidol* 27:155–161.

El-Hamamsy I, Yacoub MH (2009) Cellular and molecular mechanisms of thoracic aortic aneurysms. *Nat Rev Cardiol* 6:771–786.

Erbay E, Babaev VR, Mayers JR, Makowski L, Charles KN, Snitow ME, Fazio S, Wiest MM, Watkins SM, Linton MF, Hotamisligil GS (2009) Reducing

endoplasmic reticulum stress through a macrophage lipid chaperone alleviates atherosclerosis. *Nat Med* 15:1383–1391.

Faggion Vinholo T, Zafar MA, Ziganshin BA, Elefteriades JA (2019) Nonsyndromic Thoracic Aortic Aneurysms and Dissections—Is Screening Possible? *Semin Thorac Cardiovasc Surg* 31:628–634.

Fang CT, Kuo HH, Hsu SC, Yih LH (2019) HSP70 is required for the proper assembly of pericentriolar material and function of mitotic centrosomes. *Cell Div* 14:1–17 Available at: <https://doi.org/10.1186/s13008-019-0047-7>.

Francula-Zaninovic S, Nola IA (2018) Management of Measurable Variable Cardiovascular Disease' Risk Factors. *Curr Cardiol Rev* 14:153–163.

Frismantiene A, Philippova M, Erne P, Resink TJ (2018) Smooth muscle cell-driven vascular diseases and molecular mechanisms of VSMC plasticity. *Cell Signal* 52:48–64 Available at: <https://doi.org/10.1016/j.cellsig.2018.08.019>.

Galasso C, Lo-Castro A, Lalli C, Cerminara C, Curatolo P (2008) Neurologic Aspects of Microcephalic Osteodysplastic Primordial Dwarfism Type II. *Pediatr Neurol* 38:435–438.

Georgescu MM, Pinho M da C, Richardson TE, Torrealba J, Buja LM, Milewicz DM, Raisanen JM, Burns DK (2015) The defining pathology of the new clinical and histopathologic entity ACTA2-related cerebrovascular disease. *Acta Neuropathol Commun* 3:81.

Goodwin K, Mao S, Guyomar T, Miller E, Radisky DC, Košmrlj A, Nelson CM (2019) Smooth muscle differentiation shapes domain branches during mouse lung development. *Dev* 146.

- Griffith E, Walker S, Martin C-A, Vagnarelli P, Stiff T, Vernay B, Al Sanna N, Saggart A, Hamel B, Earnshaw WC, Jeggo P a, Jackson AP, O'Driscoll M (2008) Mutations in pericentrin cause Seckel syndrome with defective ATR-dependent DNA damage signaling. *Nat Genet* 40:232–236.
- Guey S, Tournier-Lasserre E, Herve D, Kossorotoff M (2015) Moyamoya disease and syndromes: From genetics to clinical management. *Appl Clin Genet* 8:49–68.
- Guo DC et al. (2007) Mutations in smooth muscle alpha-actin (ACTA2) lead to thoracic aortic aneurysms and dissections. *Nat Genet* 39:1488–1493.
- Guo DC et al. (2009) Mutations in Smooth Muscle Alpha-Actin (ACTA2) Cause Coronary Artery Disease, Stroke, and Moyamoya Disease, Along with Thoracic Aortic Disease. *Am J Hum Genet* 84:617–627 Available at: <http://dx.doi.org/10.1016/j.ajhg.2009.04.007>.
- Guo DC et al. (2013) Recurrent gain-of-function mutation in PRKG1 causes thoracic aortic aneurysms and acute aortic dissections. *Am J Hum Genet* 93:398–404.
- Guo DC et al. (2016) LOX mutations predispose to thoracic aortic aneurysms and dissections. *Circ Res* 118:928–934.
- Hall JG, Flora C, Scott CI, Pauli RM, Tanaka KI (2004) Majewski osteodysplastic primordial dwarfism type II (MOPD II): natural history and clinical findings. *Am J Med Genet A* 130A:55–72.
- Haneke K, Schott J, Lindner D, Hollensen AK, Damgaard CK, Mongis C, Knop M, Palm W, Ruggieri A, Stoecklin G (2019) CDK1 couples proliferation with protein synthesis. *bioRxiv* 219.

- Hansel DE, Dhara S, Huang RCC, Ashfaq R, Deasel M, Shimada Y, Bernstein HS, Harmon J, Brock M, Forastiere A, Washington MK, Maitra A, Montgomery E (2005) CDC2/CDK1 expression in esophageal adenocarcinoma and precursor lesions serves as a diagnostic and cancer progression marker and potential novel drug target. *Am J Surg Pathol* 29:390–399.
- Herrington W, Lacey B, Sherliker P, Armitage J, Lewington S (2016) Epidemiology of Atherosclerosis and the Potential to Reduce the Global Burden of Atherothrombotic Disease. *Circ Res* 118:535–546.
- Hervé D et al. (2014) Loss of $\alpha 1\beta 1$ soluble guanylate cyclase, the major nitric oxide receptor, leads to moyamoya and achalasia. *Am J Hum Genet* 94:385–394.
- Hervé D, Touraine P, Verloes A, Miskinyte S, Krivosic V, Logeart D, Alili N, Laredo JD, Gaudric A, Houdart E, Metzger JP, Tournier-Lasserre E, Woimant F (2010) A hereditary moyamoya syndrome with multisystemic manifestations. *Neurology* 75:259–264.
- Idilman IS, Ozdeniz I, Karcaaltincaba M (2016) Hepatic Steatosis: Etiology, Patterns, and Quantification. *Semin Ultrasound CT MRI* 37:501–510.
- Kamada F, Aoki Y, Narisawa A, Abe Y, Komatsuzaki S, Kikuchi A, Kanno J, Niihori T, Ono M, Ishii N, Owada Y, Fujimura M, Mashimo Y, Suzuki Y, Hata A, Tsuchiya S, Tominaga T, Matsubara Y, Kure S (2011) A genome-wide association study identifies RNF213 as the first Moyamoya disease gene. *J Hum Genet* 56:34–40.
- Kang J, Sergio CM, Sutherland RL, Musgrove EA (2014) Targeting cyclin-dependent kinase 1 (CDK1) but not CDK4/6 or CDK2 is selectively lethal to MYC-

dependent human breast cancer cells. BMC Cancer 14:1–13.

Karimi A, Milewicz DM (2016) Structure of the Elastin-Contractile Units in the Thoracic Aorta and How Genes That Cause Thoracic Aortic Aneurysms and Dissections Disrupt This Structure. Can J Cardiol 32:26–34 Available at: <http://dx.doi.org/10.1016/j.cjca.2015.11.004>.

Khera A V., Kathiresan S (2017) Genetics of coronary artery disease: Discovery, biology and clinical translation. Nat Rev Genet 18:331–344 Available at: <http://dx.doi.org/10.1038/nrg.2016.160>.

Khomich O, Ivanov A V, Bartosch B (2019) Metabolic Hallmarks of Hepatic Stellate Cells in Liver Fibrosis. Cells 9:1–22.

Kim HY, Pang MF, Varner VD, Kojima L, Miller E, Radisky DC, Nelson CM (2015) Localized Smooth Muscle Differentiation Is Essential for Epithelial Bifurcation during Branching Morphogenesis of the Mammalian Lung. Dev Cell 34:719–726 Available at: <http://dx.doi.org/10.1016/j.devcel.2015.08.012>.

Kwartler C, Zhou P, Kuang S-Q, Duan X-Y, Gong L, Milewicz D (2016) Vascular Smooth Muscle Cell Isolation and Culture from Mouse Aorta. Bio-Protocol 6:1–15.

Lehrman MA, Schneider WJ, Südhof TC, Brown MS, Goldstein JL, Russell DW (1985) Mutation in LDL receptor: Alu-Alu recombination deletes exons encoding transmembrane and cytoplasmic domains. Science (80-) 227:140–146.

Lin TS et al. (2009) Phase II study of flavopiridol in relapsed chronic lymphocytic leukemia demonstrating high response rates in genetically high-risk disease. J Clin Oncol 27:6012–6018.

- Liu W et al. (2011) Identification of RNF213 as a susceptibility gene for moyamoya disease and its possible role in vascular development. *PLoS One* 6.
- Loeys BL et al. (2006) Aneurysm Syndromes Caused by Mutations in the TGF- β Receptor. *N Engl J Med* 355:788–798.
- Logeswaran T, Friedburg C, Hofmann K, Akintuerk H, Biskup S, Graef M, Rad A, Weber A, Neubauer BA, Schranz D, Bouvagnet P, Lorenz B, Hahn A (2017) Two patients with the heterozygous R189H mutation in ACTA2 and Complex congenital heart defects expands the cardiac phenotype of multisystemic smooth muscle dysfunction syndrome. *Am J Med Genet Part A* 173:959–965.
- Mahameed M, Wilhelm T, Darawshi O, Obiedat A, Tommy WS, Chintia C, Schubert T, Samali A, Chevet E, Eriksson LA, Huber M, Tirosh B (2019) The unfolded protein response modulators GSK2606414 and KIRA6 are potent KIT inhibitors. *Cell Death Dis* 10 Available at: <http://dx.doi.org/10.1038/s41419-019-1523-3>.
- Majesky MW (2007) Developmental basis of vascular smooth muscle diversity. *Arterioscler Thromb Vasc Biol* 27:1248–1258.
- Majesky MW (2016) Vascular smooth muscle cells. *Arterioscler Thromb Vasc Biol* 36:e82–e86.
- Majesky MW (2018) Vascular development. *Arterioscler Thromb Vasc Biol* 38:E17–E24.
- Malakar AK, Choudhury D, Halder B, Paul P, Uddin A, Chakraborty S (2019) A review on coronary artery disease, its risk factors, and therapeutics. *J Cell Physiol* 234:16812–16823.
- Michel JB, Jondeau G, Milewicz DiM (2018) From genetics to response to injury:

Vascular smooth muscle cells in aneurysms and dissections of the ascending aorta. *Cardiovasc Res* 114:578–589.

Milewicz DM, Guo DC, Van Tran-Fadulu, Lafont AL, Papke CL, Inamoto S, Kwartler CS, Pannu H (2008) Genetic basis of thoracic aortic aneurysms and dissections: Focus on smooth muscle cell contractile dysfunction. *Annu Rev Genomics Hum Genet* 9:283–302.

Milewicz DM, Kwartler CS, Papke CL, Regalado ES, Cao J, Reid AJ (2010a) Genetic variants promoting smooth muscle cell proliferation can result in diffuse and diverse vascular diseases: evidence for a hyperplastic vasculomyopathy. *Genet Med* 12:196–203 Available at: <http://www.ncbi.nlm.nih.gov/pubmed/20130469>.

Milewicz DM, Ostergaard JR, Ala-Kokko LM, Khan N, Grange DK, Mendoza-Londono R, Bradley TJ, Olney AH, Ades L, Maher JF, Guo D, Buja LM, Kim D, Hyland JC, Regalado ES (2010b) De novo ACTA2 mutation causes a novel syndrome of multisystemic smooth muscle dysfunction. *Am J Med Genet Part A* 152 A:2437–2443.

Milewicz DM, Trybus KM, Guo DC, Sweeney HL, Regalado E, Kamm K, Stull JT (2017) Altered smooth muscle cell force generation as a driver of thoracic aortic aneurysms and dissections. *Arterioscler Thromb Vasc Biol* 37:26–34.

Miskinyte S, Butler MG, Hervé D, Sarret C, Nicolino M, Petralia JD, Bergametti F, Arnould M, Pham VN, Gore A V., Spengos K, Gazal S, Woimant F, Steinberg GK, Weinstein BM, Tournier-Lasserre E (2011) Loss of BRCC3 deubiquitinating enzyme leads to abnormal angiogenesis and is associated with syndromic

- moyamoya. *Am J Hum Genet* 88:718–728.
- Mizuguchi T et al. (2004) Heterozygous TGFB^{R2} mutations in Marfan syndrome. *Nat Genet* 36:855–860.
- Morisaki H, Akutsu K, Ogino H, Kondo N, Yamanaka I, Tsutsumi Y, Yoshimuta T, Okajima T, Matsuda H, Minatoya K, Sasaki H, Tanaka H, Ishibashi-Ueda H, Morisaki T (2009) Mutation of ACTA2 gene as an important cause of familial and nonfamilial nonsyndromatic thoracic aortic aneurysm and/or dissection (TAAD). *Hum Mutat* 30:1406–1411.
- Mühlhans J, Gießl A (2012) Pericentrin in health and disease: Exploring the patchwork of pericentrin splice variants. *Commun Integr Biol* 5:304–307.
- Mullassery D, Smith NP (2015) Lung development. *Semin Pediatr Surg* 24:152–155
Available at: <http://dx.doi.org/10.1053/j.sempedsurg.2015.01.011>.
- Munot P, Crow YJ, Ganesan V (2011) Paediatric stroke: Genetic insights into disease mechanisms and treatment targets. *Lancet Neurol* 10:264–274
Available at: [http://dx.doi.org/10.1016/S1474-4422\(10\)70327-6](http://dx.doi.org/10.1016/S1474-4422(10)70327-6).
- Munot P, Saunders DE, Milewicz DM, Regalado ES, Ostergaard JR, Braun KP, Kerr T, Lichtenbelt KD, Philip S, Rittey C, Jacques TS, Cox TC, Ganesan V (2012) A novel distinctive cerebrovascular phenotype is associated with heterozygous Arg179 ACTA2 mutations. *Brain* 135:2506–2514.
- Musunuru K, Kathiresan S (2019) Genetics of Common, Complex Coronary Artery Disease. *Cell* 177:132–145.
- Nakashima Y, Fujii H, Sumiyoshi S, Wight TN, Sueishi K (2007) Early human atherosclerosis: Accumulation of lipid and proteoglycans in intimal thickenings

followed by macrophage infiltration. *Arterioscler Thromb Vasc Biol* 27:1159–1165.

O'Rourke BP, Gomez-Ferreria MA, Berk RH, Hackl AMU, Nicholas MP, O'Rourke SC, Pelletier L, Sharp DJ (2014) Cep192 controls the balance of centrosome and non-centrosomal microtubules during interphase. *PLoS One* 9.

Ogura M (2018) PCSK9 inhibition in the management of familial hypercholesterolemia. *J Cardiol* 71:1–7 Available at: <http://dx.doi.org/10.1016/j.jjcc.2017.07.002>.

Owens GK, Kumar MS, Wamhoff BR (2004) Molecular Regulation of Vascular Smooth Muscle Cell Differentiation in Development and Disease. :767–801.

Palam LR, Gore J, Craven KE, Wilson JL, Korc M (2015) Integrated stress response is critical for gemcitabine resistance in pancreatic ductal adenocarcinoma. *Cell Death Dis* 6:1–13.

Papke CL, Cao J, Kwartler CS, Villamizar C, Byanova KL, Lim SM, Sreenivasappa H, Fischer G, Pham J, Rees M, Wang M, Chaponnier C, Gabbiani G, Khakoo AY, Chandra J, Trache A, Zimmer W, Milewicz DM (2013) Smooth muscle hyperplasia due to loss of smooth muscle alpha-actin is driven by activation of focal adhesion kinase, altered p53 localization and increased levels of platelet-derived growth factor receptor-beta. *Hum Mol Genet* 22:3123–3137.

Parry D, Guzi T, Shanahan F, Davis N, Prabhavalkar D, Wiswell D, Seghezzi W, Paruch K, Dwyer MP, Doll R, Nomeir A, Windsor W, Fischmann T, Wang Y, Oft M, Chen T, Kirschmeier P, Lees EM (2010) Dinaciclib (SCH 727965), a novel and potent cyclin-dependent kinase inhibitor. *Mol Cancer Ther* 9:2344–2353.

- Paruch K et al. (2010) Discovery of dinaciclib (SCH 727965): A potent and selective inhibitor of cyclin-dependent kinases. *ACS Med Chem Lett* 1:204–208.
- Pinard A, Jones GT, Milewicz DM (2019) Genetics of Thoracic and Abdominal Aortic Diseases: Aneurysms, Dissections, and Ruptures. *Circ Res* 124:588–606.
- Prabhu S, Fox S, Mattke A, Armes JE, Alphonso N (2017) Extracorporeal Life Support in Multisystem Smooth Muscle Dysfunction Syndrome. *World J Pediatr Congenit Heart Surg* 8:750–753.
- Rauch A et al. (2008) Mutations in the Pericentrin (PCNT) Gene Cause Primordial Dwarfism. *319:816–819*.
- Raymond TE, Khabbaza JE, Yadav R, Tonelli AR (2014) Significance of main pulmonary artery dilation on imaging studies. *Ann Am Thorac Soc* 11:1623–1632.
- Regalado ES et al. (2015) Aortic Disease Presentation and Outcome Associated with ACTA2 Mutations. *Circ Cardiovasc Genet* 8:457–464.
- Regalado ES, Mellor-crummey L, Backer J De, Braverman AC, Ades L, Benedict S, Bradley TJ, Brickner ME, Chatfield KC, Child A, Feist C, Holmes KW, Iannucci G, Lorenz B, Mark P, Morisaki T, Morisaki H, Morris SA (2018) Clinical history and management recommendations of the smooth muscle dysfunction syndrome due to ACTA2 arginine 179 alterations. *20*.
- Roche-Molina M, Sanz-Rosa D, Cruz FM, García-Prieto J, López S, Abia R, Muriana FJG, Fuster V, Ibáñez B, Bernal JA (2015) Induction of sustained hypercholesterolemia by single adeno-associated virus-mediated gene transfer of mutant hPCSK9. *Arterioscler Thromb Vasc Biol* 35:50–59.

- Rockey DC, Du Q, Shi Z (2019) Smooth Muscle α -Actin Deficiency Leads to Decreased Liver Fibrosis via Impaired Cytoskeletal Signaling in Hepatic Stellate Cells. *Am J Pathol* 189:2209–2220.
- Rong JX, Shapiro M, Trogan E, Fisher EA (2003) Transdifferentiation of mouse aortic smooth muscle cells to a macrophage-like state after cholesterol loading. *Proc Natl Acad Sci U S A* 100:13531–13536.
- Roskoski R (2016) Cyclin-dependent protein kinase inhibitors including palbociclib as anticancer drugs. *Pharmacol Res* 107:249–275 Available at: <http://dx.doi.org/10.1016/j.phrs.2016.03.012>.
- Roskoski R (2019) Cyclin-dependent protein serine/threonine kinase inhibitors as anticancer drugs. *Pharmacol Res* 139:471–488 Available at: <https://doi.org/10.1016/j.phrs.2018.11.035>.
- Sarkars R, Mukherjee S, Roy M (2013) Targeting heat shock proteins by phenethyl isothiocyanate results in cell-cycle arrest and apoptosis of human breast cancer cells. *Nutr Cancer* 65:480–493.
- Schmitt E, Paquet C, Beauchemin M, Bertrand R (2007) DNA-damage response network at the crossroads of cell-cycle checkpoints, cellular senescence and apoptosis. *J Zhejiang Univ Sci B* 8:377–397.
- Schuetz A, Nana D, Rose C, Zocher G, Milanovic M, Koenigsmann J, Blasig R, Heinemann U, Carstanjen D (2011) The structure of the Klf4 DNA-binding domain links to self-renewal and macrophage differentiation. *Cell Mol Life Sci* 68:3121–3131.
- Scott RM, Smith ER (2009) Moyamoya Disease and Moyamoya Syndrome. *N Engl J*

Med 360:1226–1237.

Seol HJ, Shin DC, Kim YS, Shim EB, Kim S-K, Cho B-K, Wang K-C (2010)

Computational analysis of hemodynamics using a two-dimensional model in moyamoya disease. *J Neurosurg Pediatr* 5:297–301 Available at: <http://www.ncbi.nlm.nih.gov/pubmed/20192649>.

Shankman LS, Gomez D, Cherepanova OA, Salmon M, Alencar GF, Haskins RM, Swiatlowska P, Newman AAC, Greene ES, Straub AC, Isakson B, Randolph GJ, Owens GK (2015) KLF4-dependent phenotypic modulation of smooth muscle cells has a key role in atherosclerotic plaque pathogenesis. *Nat Med* 21:628–637.

Sharma B, Chang A, Red-Horse K (2017) Coronary Artery Development: Progenitor Cells and Differentiation Pathways. *Annu Rev Physiol* 79:1–19.

Soria LF, Ludwig EH, Clarke HRG, Vega GL, Grundy SM, McCarthy BJ (1989) Association between a specific apolipoprotein B mutation and familial defective apolipoprotein B-100. *Proc Natl Acad Sci U S A* 86:587–591.

Tabas I, García-Cardena G, Owens GK (2015) Recent insights into the cellular biology of atherosclerosis. *J Cell Biol* 209:13–22.

Taubenslag KJ, Scanga HL, Huey J, Lee J, Medsinge A, Sylvester CL, Cheng KP, Nischal KK (2019) Iris anomalies and the incidence of ACTA2 mutation. *Br J Ophthalmol* 103:499–503.

Tibelius A, Marhold J, Zentgraf H, Heilig CE, Neitzel H, Ducommun B, Rauch A, Ho AD, Bartek J, Kramer A (2009) Microcephalin and pericentrin regulate mitotic entry via centrosome-associated Chk1. *J Cell Biol* 185:1149–1157.

- Udan RS, Culver JC, Dickinson ME (2013) Understanding vascular development. Wiley Interdiscip Rev Dev Biol 2:327–346.
- van der Graaff D, Kwanten WJ, Francque SM (2019) The potential role of vascular alterations and subsequent impaired liver blood flow and hepatic hypoxia in the pathophysiology of non-alcoholic steatohepatitis. Med Hypotheses 122:188–197.
- Vazquez REZ, Coetzee A, Harlock E, Simmerson M, Cohen MC (2015) Measurement of nucleated red blood cells in the peripheral blood as a marker of hypoxia in sudden unexpected death in infancy. J Clin Pathol 68:718–722.
- Wagenseil JE, Mecham RP (2009) Vascular extracellular matrix and arterial mechanics. Physiol Rev 89:957–989.
- Wang D, Uhrin P, Mocan A, Waltenberger B, Breuss JM, Tewari D, Mihaly-Bison J, Huminiecki Ł, Starzyński RR, Tzvetkov NT, Horbańczuk J, Atanasov AG (2018) Vascular smooth muscle cell proliferation as a therapeutic target. Part 1: molecular targets and pathways. Biotechnol Adv 36:1586–1607.
- Ward NC, Watts GF, Eckel RH (2019) Statin Toxicity: Mechanistic Insights and Clinical Implications. Circ Res 124:328–350.
- Willems M et al. (2009) Molecular analysis of pericentrin gene (PCNT) in a series of 24 Seckel/microcephalic osteodysplastic primordial dwarfism type II (MOPD II) families. J Med Genet 47:797–802.
- Williams KJ, Tabas I (1995) The response-to-retention hypothesis of early atherogenesis. Arterioscler Thromb Vasc Biol 15:551–562.
- Wirka RC et al. (2019) Atheroprotective roles of smooth muscle cell phenotypic

modulation and the TCF21 disease gene as revealed by single-cell analysis.

Nat Med 25:1280–1289 Available at: <http://dx.doi.org/10.1038/s41591-019-0512-5>.

Xue F, Lu J, Buchl SC, Sun L, Shah VH, Malhi H, Maier JL (2021) Coordinated Signaling of Activating Transcription Factor 6 α and Inositol Requiring Enzyme 1 α Regulates Hepatic Stellate Cell-Mediated Fibrogenesis in Mice. *Am J Physiol Liver Physiol*.

Yang JQ, Liu HX, Liang Z, Sun YM, Wu M (2014) Over-expression of p53, p21 and cdc2 in histologically negative surgical margins is correlated with local recurrence of laryngeal squamous cell carcinoma. *Int J Clin Exp Pathol* 7:4295–4302.

Yoshikawa A, Sato S, Tanaka T, Hashisako M, Kashima Y, Tsuchiya T, Yamasaki N, Nagayasu T, Yamamoto H, Fukuoka J (2016) Breakdown of lung framework and an increase in pores of kohn as initial events of emphysema and a cause of reduction in diffusing capacity. *Int J COPD* 11:2287–2294.

Yu S, Mceniery CM (2020) Central Versus Peripheral Artery Stiffening and Cardiovascular Risk. *Arterioscler Thromb Vasc Biol*:1028–1033.

Zeidner JF, Foster MC, Blackford AL, Litzow MR, Morris LE, Strickland SA, Lancet JE, Bose P, Yair Levy M, Tibes R, Gojo I, Gocke CD, Rosner GL, Little RF, Wright JJ, Austin Doyle L, Douglas Smith B, Karp JE (2015) Randomized multicenter phase II study of flavopiridol (alvocidib), cytarabine, and mitoxantrone (FLAM) versus cytarabine/daunorubicin (7+3) in newly diagnosed acute myeloid leukemia. *Haematologica* 100:1172–1179.

- Zhang L, Kang W, Lu X, Ma S, Dong L, Zou B (2018) LncRNA CASC11 promoted gastric cancer cell proliferation, migration and invasion in vitro by regulating cell cycle pathway. *Cell Cycle* 17:1886–1900 Available at: <https://doi.org/10.1080/15384101.2018.1502574>.
- Zhou AX, Wang X, Lin CS, Han J, Yong J, Nadolski MJ, Borén J, Kaufman RJ, Tabas I (2015) C/EBP-Homologous protein (CHOP) in vascular smooth muscle cells regulates their proliferation in aortic explants and atherosclerotic lesions. *Circ Res* 116:1736–1743.
- Zhou Z, Peters AM, Wang S, Janda A, Chen J, Zhou P, Arthur E, Kwartler CS, Milewicz DM (2019) Reversal of aortic enlargement induced by increased biomechanical forces requires AT1R inhibition in conjunction with AT2R activation. *Arterioscler Thromb Vasc Biol* 39:459–466.
- Zhu L, Vranckx R, Van Kien PK, Lalande A, Boisset N, Mathieu F, Wegman M, Glancy L, Gasc JM, Brunotte F, Bruneval P, Wolf JE, Michel JB, Jeunemaitre X (2006) Mutations in myosin heavy chain 11 cause a syndrome associating thoracic aortic aneurysm/aortic dissection and patent ductus arteriosus. *Nat Genet* 38:343–349.
- Zimmerman WC, Sillibourne J, Rosa J, Doxsey SJ (2004) Mitosis-specific Anchoring of gamma Tubulin Complexes by Pericentrin Controls Spindle Organization and Mitotic Entry. *Mol Biol Cell* 15:3751–3737.

Vita

Jamie Mae Wright was born on September 5, 1987. She is the daughter of James and Kathleen Wright. She graduated valedictorian from The Colony High School in 2006. She went on to complete a Bachelor of Science in Molecular Biology with a minor in Neurobiology at the University of Texas at Dallas where she graduated *summa cum laude* in May 2010. For the next year she worked as a research technician in the Department of Developmental Biology at the University of Texas Southwestern Medical Center. She began the combined MD/PhD program at the University of Texas Health Science Center in Houston in May 2011. She will graduate with a Doctorate in Medicine and a Doctorate in Philosophy in June 2021.

Permanent address:

5124 Runyon Dr.
The Colony, TX 75056

Email: jamie.wright0610@gmail.com